Electronic Supplementary Material (ESI) for Green Chemistry.

Supporting Information

Enzymatic degradation of synthetic polyisoprenes via surfactant-free polymer emulsification

Table of content

1. Materials and methods

Chemicals. Ethyl acetate, *n*-hexane and dichloromethane were purchased in technical grade and distilled before further use. Methanol was used in LC-MS grade from VWR and as Chromasolv™ for UHPLC-ESI-HRMS from Honeywell Riedel de Haën™. Acetone was used in HPLC grade from Sigma Aldrich. Sodium iodide was purchased from Sigma Aldrich. Potassium phosphate buffer was freshly prepared using MilliQ-water, potassium hydrogen phosphate from Th. Geyer and potassium dihydrogen phosphate from Roanal. The *n*-hexadecane was purchased from Fluka. Formic acid for LC-MS was purchased as LiChropur® from Merck. The synthetic polyisoprenes were provided by Trinseo Deutschland GmbH. The naturally derived polyisoprene was purchased from Sigma Aldrich and precipitated in methanol from dichloromethane prior to use. Latex milk with a low ammonia concentration was provided by Weber and Schaer GmbH & Co. KG. An auto-induction TB medium for enzyme expression with trace elements from Formedium was used for enzyme expression.

UHPLC. Chromatographic analysis was performed using a Waters Acquity UPLC system equipped with a UV-detector. The RP-C8 UHPLC column from Agilent (InfinityLab Poroshell 120 EC-C8, 2.1 x 50 mm, 1.9 µm) with a guard column (InfinityLab Poroshell 120 EC-C8, 2.1 mm, 1.9 µm) was used. The mobile phases were water (A) and MeOH (B). Chromatographic separation of the samples (injection volume 5 µL) was realized using a gradient system starting from 68% B (isocratic for 0.5 min) and increasing to 100% B within 2 min, followed by further 3.5 min at 100% B at a flow rate of 0.7 mL/min. Then the flow rate was increased within 1 min to 1 mL/min holding at 100% B for further 9 min. The column re-equilibration time was set to 3 min at 68% B (flow 0.7 mL/min). The oven temperature was set at 35 °C and the analytes were detected at 210 nm.

ESI-TOF-MS. ESI-TOF-MS measurements were performed on a Bruker Daltonics microTOF via direct injection at a flow rate of 180 µL h^{-1} in positive mode with an acceleration voltage of 4.5 kV. Samples were prepared by dissolving in LC-MS grade methanol with additional sodium iodide salt in acetone. The software Data Analysis (version 4.0) was used for data evaluation.

UHPLC-UV-ESI-HRMS (QTOF). The UHPLC-UV-ESI-HRMS measurements were performed with a TripleToF 6600-1 mass spectrometer (Sciex), which was equipped with an ESI-DuoSpray-Ion-Source (it operated in positive ion mode) and was controlled by Analyst 1.7.1 TF software (Sciex). The ESI source operation parameters were as follows: ion spray voltage: 5,500 V, nebulizing gas: 75 p.s.i., source temperature: 450 °C, drying gas: 60 p.s.i., curtain gas: 55 p.s.i. Data acquisition was performed in the MS1-ToF mode, scanned from 100 to 1500 Da with an accumulation time of 250 ms. The instrument was externally calibrated by the ESI positive ion calibration solution from Sciex. The MS system was coupled to an ultra-high-performance liquid chromatography (UHPLC) system (Waters I-class, Waters), equipped with a RP-8 column (particle size 1.9 µm, 50 × 2.1 mm ID, InfinityLab Poroshell 120 EC-C8, Agilent; column temperature 45 °C) with a guard column (InfinityLab Poroshell 120 EC-C8, 2.1 mm, 1.9 µm). The mobile phases were H_2O (A; MilliQ-biocel apparatus from Millipore (Billerica, USA)) and MeOH (B; Chromasolv™, for LC-MS, Honeywell Riedel de Haën™), each with 0.1% formic acid (additive for LC-MS, LiChropur®, Merck). Chromatographic separation of the samples (injection volume 10 µL) was realized using a gradient system starting from 70% B (isocratic for 1 min) and increasing to 100% B within 3 min, followed by further 3 min at 100% B at a flow rate of 0.3 mL/min. Then the flow rate was increased within 0.5 min to 0.4 mL/min holding at 100% B for further 3.5 min. The column re-equilibration time was set to 3 min at 70% B (flow 0.3 mL/min). The wavelength range of the PDA measurements was 200-600 nm used for detection. The data were evaluated using the software Peakview 1.2.0.3 (AB Sciex).

UHPLC-ESI-HRMS. The positive ion high-resolution ESI mass spectra (*m/z* range 150-1500) were obtained with an Orbitrap Elite mass spectrometer (Thermo Fisher Scientific, Germany) equipped with a heated electrospray ion source (spray voltage 3.8 kV, capillary temperature 325 °C, source heater temperature 300 °C, FTMS resolution 30.000). Nitrogen was used as a sheath and auxiliary gas. The MS system was coupled to an ultra-high-performance liquid chromatography (UHPLC) system (Dionex UltiMate 3000, Thermo Fisher Scientific), equipped with a RP-8 column (particle size 1.9 µm, 50 × 2.1 mm ID, InfinityLab Poroshell 120 EC-C8, Agilent; column temperature 40 °C) with a guard column (InfinityLab Poroshell 120 EC-C8, 1.9 µm, 2.1 mm ID). The mobile phases were H_2O (A; MilliQ-biocel apparatus from Millipore (Billerica, USA)) and MeOH (B), each with 0.1% formic acid (additive for LC-MS). Chromatographic separation of the samples (injection volume 5 µL) was realized using a gradient system starting from 70% B (isocratic for 1 min) and increasing to 100% B within 3 min, followed by further 3 min at 100% B at a flow rate of 0.3 mL/min. Then the flow rate was increased within 0.5 min to 0.4 mL/min holding at 100% B for further 3.5 min. The column re-equilibration time was set to 3 min at 70% B (flow 0.3 mL/min). High energy collision dissociation (HCD) mass spectra were recorded at a relative collision energy

of 40 % using nitrogen as the collision gas. The instrument was calibrated externally using the Pierce ESI positive ion calibration solution (product no. 88323) from Thermo Fisher Scientific. The data were evaluated using the software Xcalibur 2.2 SP1.

Dynamic light scattering (DLS). The size distributions of the emulsions were determined on an Anton-Paar Litesizer 500. Samples were measured with a measurement angle of 175° and a focus position of -3.707 mm. A series of 6 runs with disposable measuring cells and 25 °C temperature was evaluated. A refractive index of 1.33 for the utilized dispersant was applied. Transmittance was determined under the same conditions using the Litesizer 500. The data were evaluated using the software Kalliope™.

Zeta potential measurement. The zeta potentials of the emulsions were determined on an Anton-Paar Litesizer 500 with omega cuvettes. Smoluchowski Approximation and Henry factor of 1.5 were applied. A relative permittivity of 78 was applied for the dispersant 0.1 mM KCl used.

NMR. The ^{1}H NMR spectra were measured using an Agilent Technologies 400 MHz VNMRS and 500 MHz DD2 at 27°C. Chemical shifts (δ) are reported in ppm and referred to the residual solvent signal ($CDCl_3$ 7.26 ppm for ^{1}H).

Ultrasonication. Ultrasound treatments for the acoustically emulsified system were performed with a VCX 500 ultrasonic processor (Sonics & Materials, CT, USA) equipped with a 3 mm micro tip. Cycles of pulsed ultrasound at a frequency of 20 kHz were applied using 20% of the maximum amplitude with a sequence of 10 s pulse and 5 s pause for 30 minutes were applied.

Sonication. Co-solvent stabilized systems were sonicated in an ultrasonic cleaner (VWR) filled with MilliQ-water at an ultrasound frequency of 45 kHz.

Gel permeation chromatography (GPC). Tetrahydrofuran-based SEC measurements were performed at 30 °C on a Viscotek GPCmax VE 2001 from ViscotekTM using a CLM3008 precolumn and a CLM3008 main column. THF was used as the solvent while applying a flow rate of 1 $mL \cdot min^{-1}$. To determine the molecular weights, the refractive index of the sample under study was determined using a VE 3580 RI detector of ViscotekTM. External calibration was performed using poly(styrene) (PS) standards (purchased from PSS) with a molecular weight range from 1050 to 115000 g mol-1. OmniSEC software (Version 4.6.2.359) was used to analyze the data.

Light microscopy. Light microscopy images were obtained using Axiolab from Carl Zeiss.

Refractive index measurement. Refractive index was determined on an Anton-Paar Litesizer 500 using quartz cuvettes and MilliQ-water as a reference.

Transmission electron microscopy (TEM). TEM studies were carried out using an EM 900 transmission electron microscope from Carl Zeiss Microscopy GmbH.

2. Experimental procedures

Degradation experiments:

Preparation of non-emulsified system

Polyisoprene (0.2 wt/vol%) was placed in a 5 mL vial. Potassium phosphate solution (5 mM) was freshly prepared and added to the reaction vial. The mixture was stirred vigorously before the addition of the Lcp_{K30} enzyme (5 μM). After the addition of the enzyme, the vials were sealed with parafilm to prevent the evaporation of solvent. The reaction was carried out at room temperature with the exclusion of light for 24 hours at a stirring speed of 450 rpm. Ethyl acetate (1.5 mL) was added, sonicated for 10 minutes and stirred for 30 minutes for liquid-liquid extraction. The hydrophobic phase was isolated with a syringe and 1 mL was used for further analysis. The solvent was evaporated with dried air and then the residue was redissolved in methanol and used for UHPLC, ESI-TOF-MS and UHPLC-(UV)-ESI-HRMS analysis. Negative control samples were prepared as described above without addition of the enzyme Lcp_{K30}.

Preparation of acoustically emulsified system

Polyisoprene (0.2 wt/vol%) was placed in a pressure vial. Potassium phosphate solution (5 mM) was freshly prepared and added to the reaction vial and then pre-emulsified with vigorous stirring. Emulsification was achieved by sonication at 20% amplitude for 30 minutes, 5 seconds of pulse and 10 seconds of pause under constant cooling in a sodium chloride-ice bath. The emulsion (0.2 wt/vol%) was transferred to 5 mL vials and then the enzyme Lcp_{K30} (5 µM) was added afterwards. Evaporation of the solvent was prevented by sealing the vial with parafilm. The reaction was carried out at room temperature excluding light for 24 hours with stirring of 450 rpm. For liquid-liquid extraction, ethyl acetate (1.5 mL) was added, sonicated and stirred for 30 minutes. The hydrophobic phase was isolated with a syringe and 1 mL was used for further analysis. The solvent was evaporated with dried air and then the residue was redissolved in methanol and used for UHPLC, ESI-TOF-MS and UHPLC-(UV)-ESI-HRMS analysis. Negative control samples were prepared as described above without addition of the enzyme Lcp_{K30}.

Preparation of co-solvent stabilized system

Polyisoprene (0.2 wt/vol%) was placed into a 5 mL vial and then *n*-hexadecane (0.2 wt/vol%) was added, forming a hydrophobic phase. The mixture was stirred vigorously to dissolve the polymer in the hydrophobic phase. Potassium phosphate solution (5 mM) was freshly prepared and added to the reaction vial. The mixture was then vigorously stirred and sonicated for 1 h. Lcp_{K30} (5 µM) was added and the vials were sealed with parafilm to prevent evaporation of solvent. The reaction was carried out at room temperature excluding light for 24 hours with stirring of 450 rpm. For liquid-liquid extraction, ethyl acetate (1.5 mL) was added, sonicated and stirred for 30 minutes. The hydrophobic phase was isolated with a syringe and 1 mL was used for further analysis. The solvent was evaporated with dried air and then the residue was redissolved in methanol and used for UHPLC, ESI-TOF-MS and UHPLC-(UV)-ESI-HRMS analysis. Negative control samples were prepared as seen above without addition of enzyme Lcp_{K30}.

Stability assay

Emulsions and corresponding controls (individual components, buffer only) were prepared as described above. The reaction was started by adding 5 µM Lcp_{K30} and stirred at 450 rpm. 50 µl samples were taken at different time points and added to 950 µL of 0.2% (w/v) latex milk in 20 mM KPi buffer (pH 7). These secondary activity samples were shaken at 800 rpm and 37°C for 1.5 hours. The activity assay was terminated by extraction with 1 mL ethyl acetate. In order to achieve a clear phase separation samples were centrifuged at 14500 rpm for 5 min. 700 µL of the organic phase was transferred into a new 1.5 mL reaction tube, evaporated in a vacuum centrifuge and redissolved in 700 µl acetonitrile. The samples were analysed by UHPLC.

Amino acid sequence of Lcp_{K30}

The used latex-clearing protein Lcp_{K30} from *Streptomyces* sp. K30 is cloned into the pAGM22082-N[1] vector with an N-terminal Strep-tag and TEV protease cleavage site, a C-terminal linker and GFP11-tag[2].

MWSHPQFEKENLYFQGLQRPLWTWSPSASVAGTGVGVDPEYVWDEEADPVLAAVIDRGEVPAVNALLKQWTRNDQALPG
GLPGDLREFMEHARRMPSWADKAALDRGAQFSKTKGIYVGALYGLGSGLMSTAIPRESRAVYYSKGGADMKDRIAKTARLGY
DIGDLDAYLPHGSMIVTAVKTRMVHAAVRHLLPQSPAWSQTSGGQKIPISQADIMVTWHSLATFVMRKMKQWGVRVNTAD
AEAYLHVWQVSAHMLGVSDEYIPATWDAANAQSKQVLDPILAHTPEGEALTEVLLGIVAELDAGLTRPLIGAFSRYTLGGEVGD
MIGLAKQPVLERLIATAWPLLVAFREGLIPLPAVPAVLWTLEEALRKFVLLFLSEGRRIAIDIPDVNRPSDGGSGGGSTSRDHMVL
HEYVNAAGIT

Protein expression

Lcp_{K30} was expressed in *E. coli* BL21(DE3) cells. 4x 500 mL auto-induction TB medium (50 µg/mL kanamycin, 100 µM $FeCl_3$, 100 µM 5-aminolevulinic acid) in 2.5 L baffled Erlenmeyer flasks were inoculated 1:100 with an overnight grown pre-culture. The main culture was cultivated at 37°C and 120 rpm for 4 hours. Then the expression temperature was reduced to 25°C and the cultivation was continued for another 24 h. Cells were harvested by centrifugation at 3000 g for 30 min at 4°C.

Protein purification

Cell pellets were resuspended in lysis buffer (100 mM KPi pH 7.7; 150 mM NaCl, 1 mg/mL lysozyme, 100 µg/mL DNAse I), homogenized by sonication (Bandelin Sonoplus HD3100: 3x30 s, 70 % amplitude, pulse mode) and lysed using a cell disruptor (2 cycles, 1,3 kbar, model TS2, Constant Systems Ltd, Daventry, United Kingdom). After centrifugation (15500 g, 4 °C, 20 min) the cleared cell extract was applied onto a 5 mL Strep-Tactin®XT gravity flow column (IBA GmbH, Göttingen, Germany). Unbound protein was washed out with 5x5 mL binding buffer (100 mM KPi pH 7,7; 150 mM NaCl) and the protein of interest was eluted with 6x2 mL of binding buffer containing 50 mM biotin.
For buffer exchange PD-10 columns were used according to the manufacturer's protocol (GE Healthcare Europe GmbH, Freiburg, Germany). 20 mM KPi pH 7 was used as storage buffer. Samples were then flash frozen in liquid nitrogen and stored at -20 °C. The concentration of purified Lcp_{K30} was determined by absorbance at 412 nm (ε=80000 M-1 cm-1)[3].

3. Characterization of the emulsification system

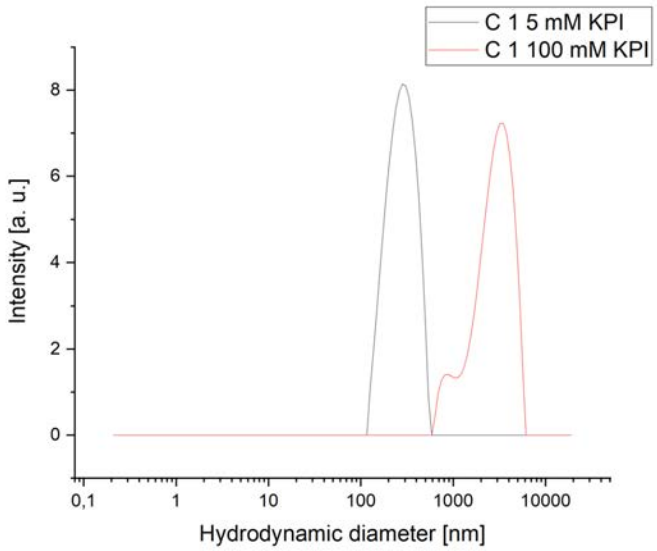

Figure S1. KPI concentration dependency on emulsions of C 1. Stacked dynamic light measurements of C 1 in KPi 5mM (black) with C 1 in KPi 100 mM (red) according to intensity.
Broadening of the hydrodynamic diameter of the emulsions at increased KPi concentrations.

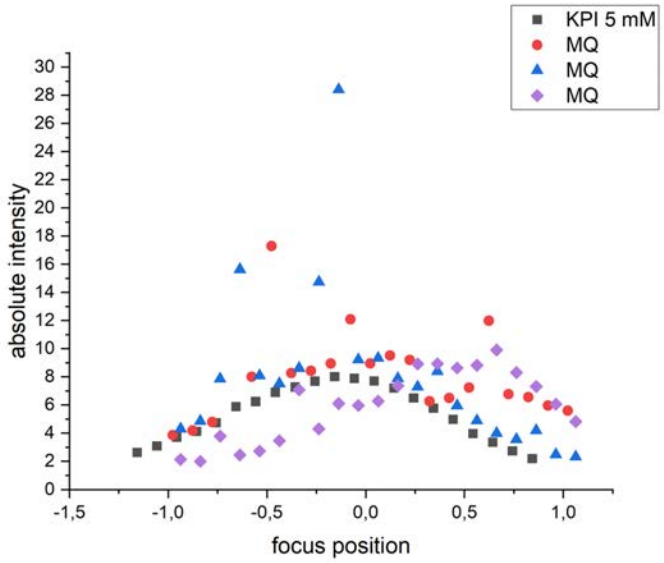

Figure S2. Refractive index determination of KPi 5 mM.

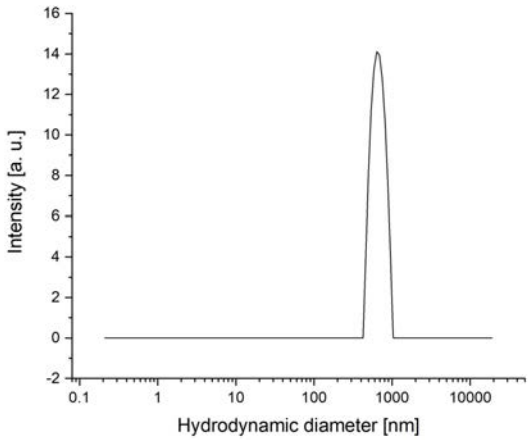

Figure S3. Dynamic light scattering (DLS) of latex milk sample L 1 with a hydrodynamic diameter of 750 nm.

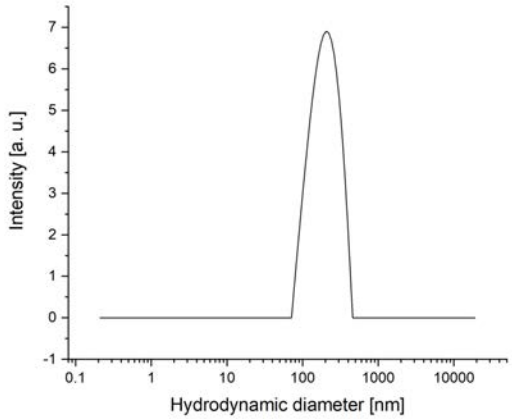

Figure S4. DLS of the negative control of the co-solvent emulsified C 1/2 (NC), *n*-hexadecane in KPi 5 mM, with a hydrodynamic diameter of 190 nm.

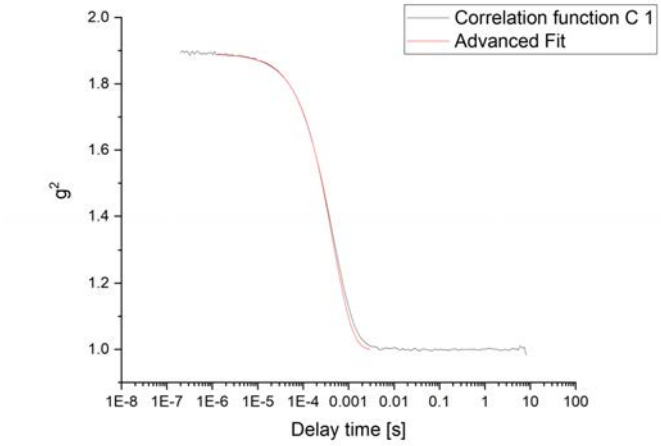

Figure S5. Correlation Function (black) with fit (red) of the dynamic light scattering measurement of the co-solvent emulsified system C 1 in KPi 5 mM.

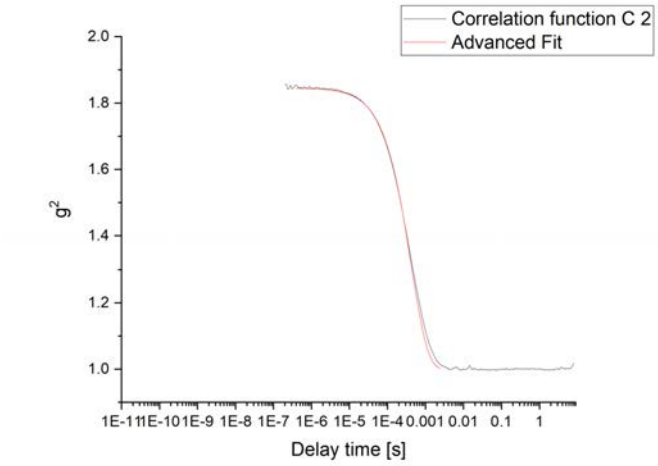

Figure S6. Correlation Function (black) with fit (red) of the dynamic light scattering measurement of the co-solvent emulsified system C 2 in KPi 5 mM.

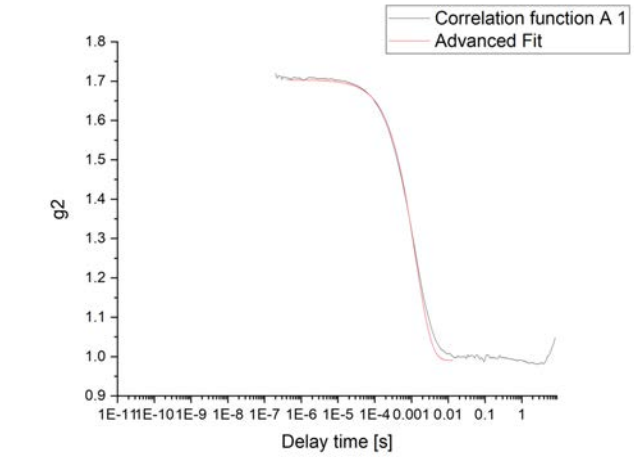

Figure S7. Correlation Function (black) with fit (red) of the dynamic light scattering measurement of the acoustically emulsified system A 1 in KPi 5 mM.

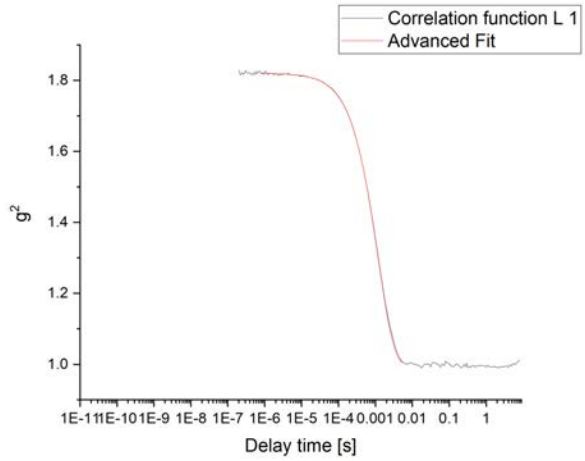

Figure S8. Correlation Function (black) with fit (red) of the dynamic light scattering measurement of the latex milk L 1 in KPi 5 mM.

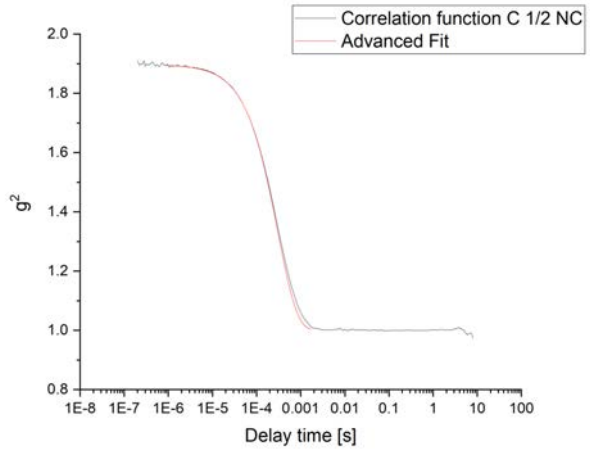

Figure S9. Correlation Function with fit of the dynamic light scattering measurement of the negative control of C 1-2 in KPi 5 mM.

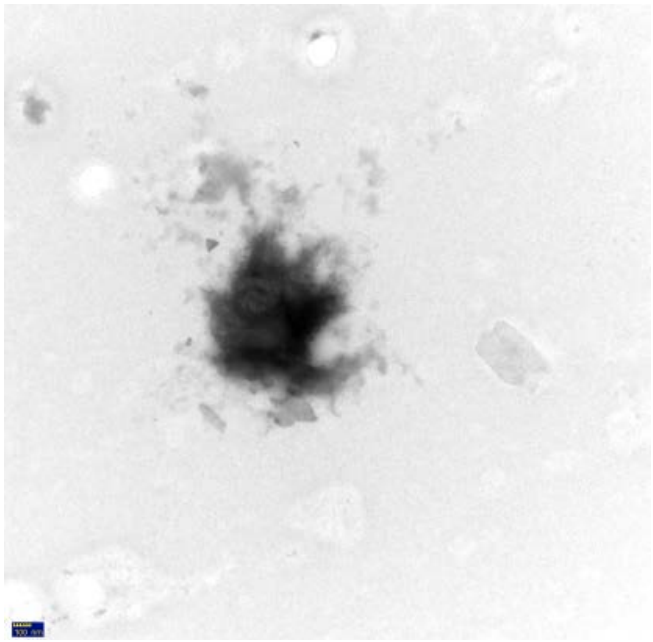

Figure S10. TEM image of acoustically emulsified PI 3000 (A 1) as micrometer-sized polyisoprene droplet. PI 3000 as A1 was dispersed but no supramolecular structure can be determined.

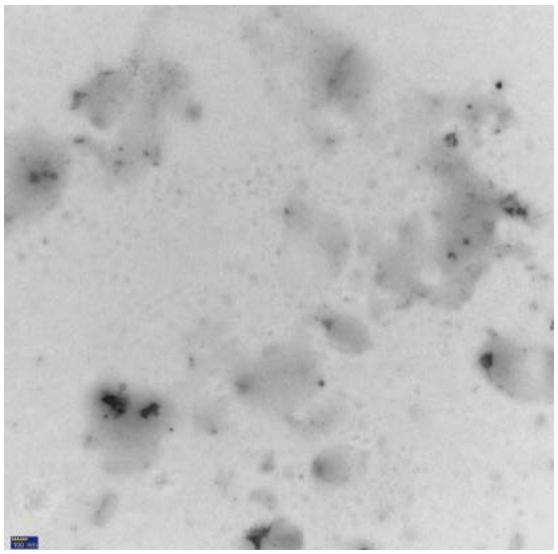

Figure S11. TEM image of co-solvent stabilized PI 3000 (C1).
PI 3000 as C1 was dispersed but no supramolecular structure can be determined.

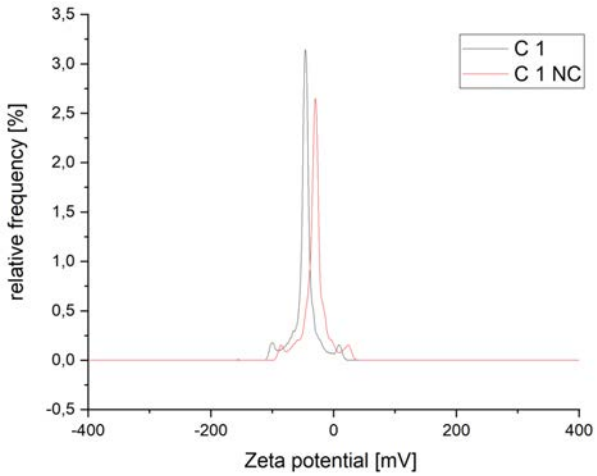

Figure S12. Stabilization increase determination of system from C1 (NC), *n* -hexadecane in MilliQ-Water, -35 mV to C1, co-solvent stabilized PI 3000, -47 mV by zeta potential measurement.

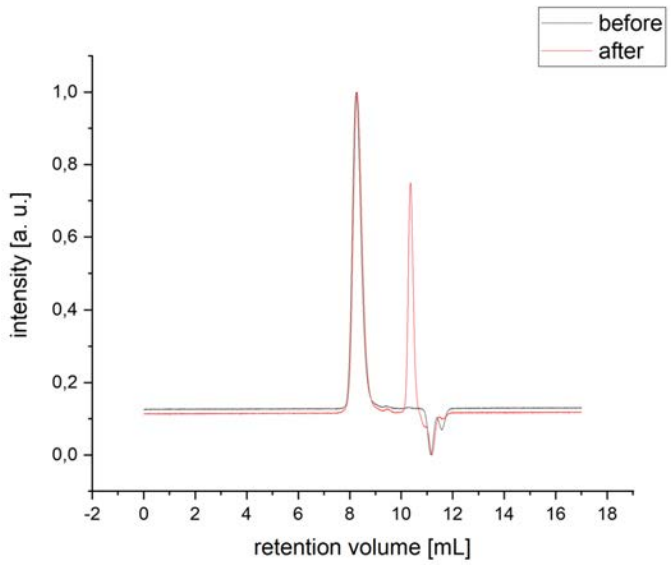

Figure S13. GPC curves of the polymer PI 3000 before (black) and after (red) ultra-sonication.

The sample was freeze-dried after ultra-sonication in water and then measured in tetrahydrofuran. Residual water solvent peak starts at 10 mL. This shows that the polymer is not affected by the ultrasonication procedure as described above.

4. Enzyme and degradation characteristics

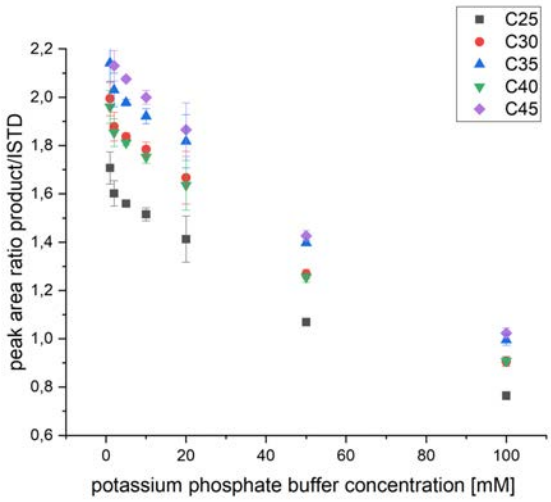

Figure S14. Oligoisoprenoidic degradation fragment dependency of KPi concentration investigated using UV-UHPLC measurements. Triplicates to determine the standard deviation.

Metastable hydrocarbon-polymer in water systems as the one we envisioned are more polydisperse in the presence of buffers, which are necessary for the stability of the enzyme in itself, as seen in our preliminary investigations (Figure S1). Consequently, we investigated an activity maximum of potassium phosphate for the degradation of natural polyisoprene to assure that the balance of interacting effects can be minimized. Rubber oxygenases are heme-containing enzymes and oxidatively cleave polyisoprene to low molecular weight oligoisoprenoids with terminal aldehyde and keto groups between a variable number of intact isoprene units, depending on the type of rubber oxygenase[4]. These oligoisoprenoidic fragments were tracked with the distinct degradation pattern of the enzyme Lcp_{K30} [5] via UHPLC and compared at different potassium phosphate buffer concentrations (Figure S9) and showed an optimum for the oligoisoprenoidic degradation fragments in question

at 1 mM KPi. The most commonly used concentrations of buffer in the degradation of *cis*-1,4-polyisoprene is 100 mM KPI for Lcp_{K30}[4]. A KPI concentration of 5 mM was used to assure enzyme stability for prolonged time.

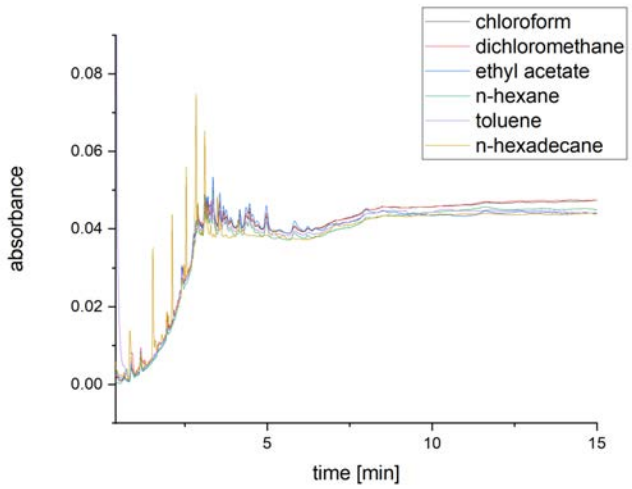

Figure S15. Degradation inhibition of the enzymatic degradation of PI cis 7000 by different solvents. Stacked UHPLC curves with gradient of six degradations runs with PI *cis* 7000 in the presence of chloroform (black), dichloromethane (red), ethyl acetate (blue), *n*-hexane (green), toluene (purple) and *n*-hexadecane (light brown). UHPLC was conducted at conditions as seen above.

Comparison of the effect of solvents onto degradation capabilities of the enzyme Lcp_{K30} indicates the least inhibition for the degradation in the presence of the solvent *n*-hexadecane.

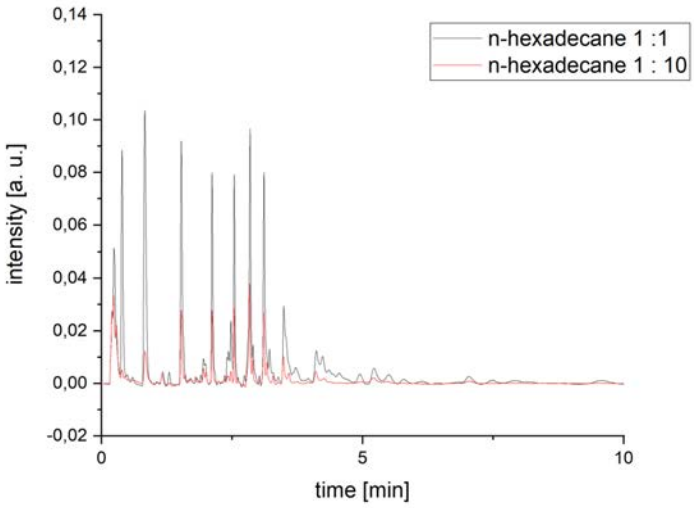

Figure S16. Degradation inhibition by *n*-hexadecane at different ratios. Stacked UHPLC curves of two degradations runs with weight ratios of PI *cis* 7000: *n*-hexadecane of 1:1 (black) and 1:10 (red). UHPLC was conducted at conditions as seen above.

This indicated higher enzyme degradation inhibition at weight ratios of 1:10 (PI cis 7000: *n*-hexadecane) than for 1:1 (PI cis 7000: *n*-hexadecane).

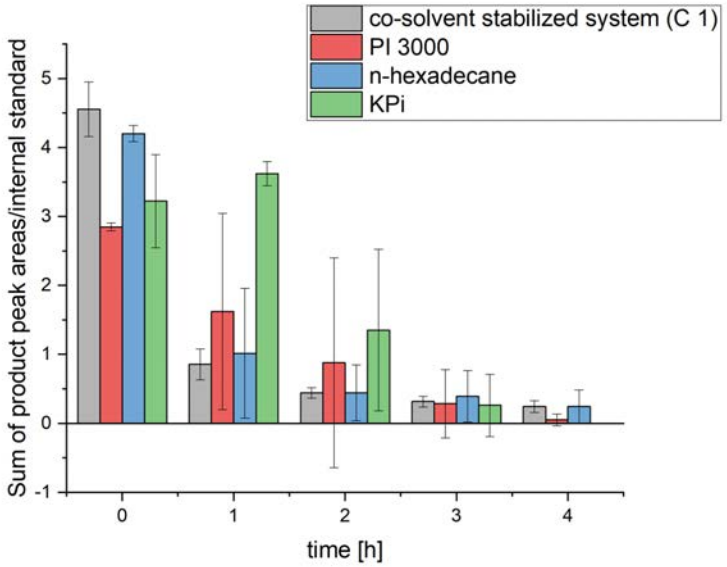

Figure S17. Enzyme stability with emulsion, polyisoprene, *n*-hexadecane and KPI buffer at 700 rpm. Co-solvent stabilized system (C 1) (grey), polyisoprene PI 3000 (red), *n*-hexadecane (blue) and potassium phosphate buffer (KPi) (green). Triplicates to determine the standard deviation.

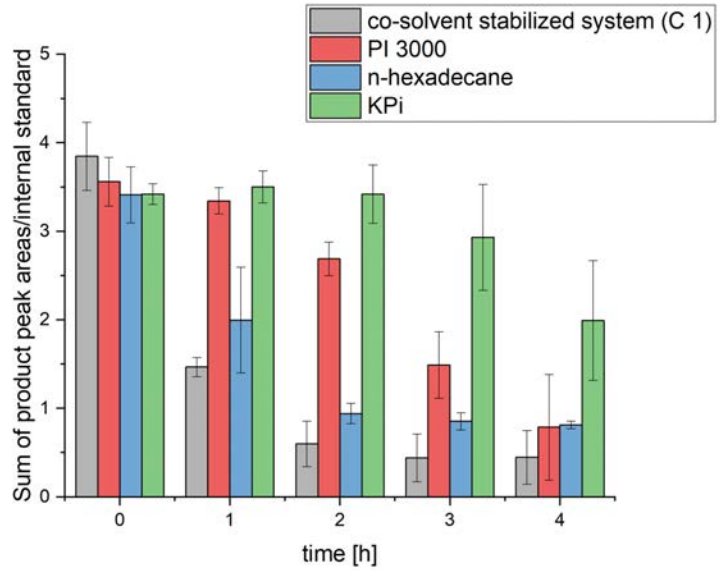

Figure S18. Enzyme stability with emulsion, polyisoprene, *n*-hexadecane and KPI buffer at 450 rpm. Co-solvent stabilized system (C 1) (grey), polyisoprene PI 3000 (red), *n*-hexadecane (blue) and potassium phosphate buffer (KPi) (green). Triplicates to determine the standard deviation.

The stirring speed had a significant effect on the enzymatic degradation capabilities of Lcp_{K30} and was optimized accordingly.

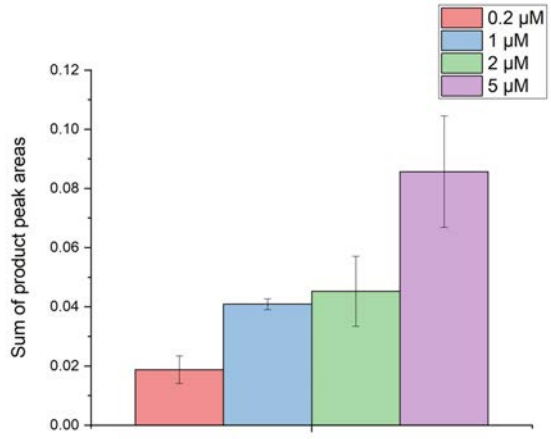

Figures S19. Enzymatic degradations of PI 3000 at different enzyme loadings measured using UV-UHPLC measurements. Enzyme concentrations of 0.2 µM (red), 1 µM (blue), 2 µM (green) and 5 µM (purple). Triplicates to determine the standard deviation.

The sum area of product peaks of the enzymatic degradation of synthetic polyisoprene PI 3000 were determined via integration of UV-UHPLC chromatograms and the subtraction of the background with negative controls, without the addition of enzyme Lcp_{K30}. The sum of product peak area increased with the loading of the enzyme Lcp_{K30}.

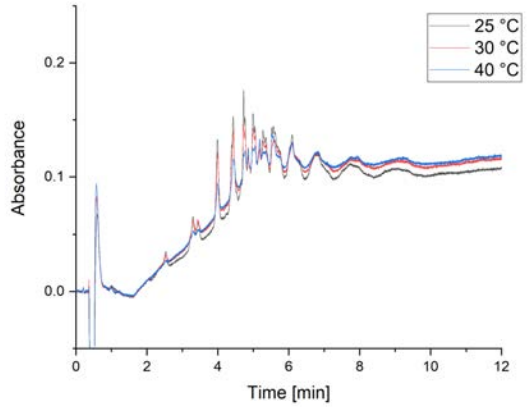

Figure S20. Stacked UV-UHPLC chromatograms, with gradient, of the enzymatic degradation of PI 3000 at 25 °C (black), 30 °C (red) and 40 °C (blue).

Increasing the temperature did not lead to more degradation products according to UHPLC analysis. Consequently, the reactions were conducted at room temperature.

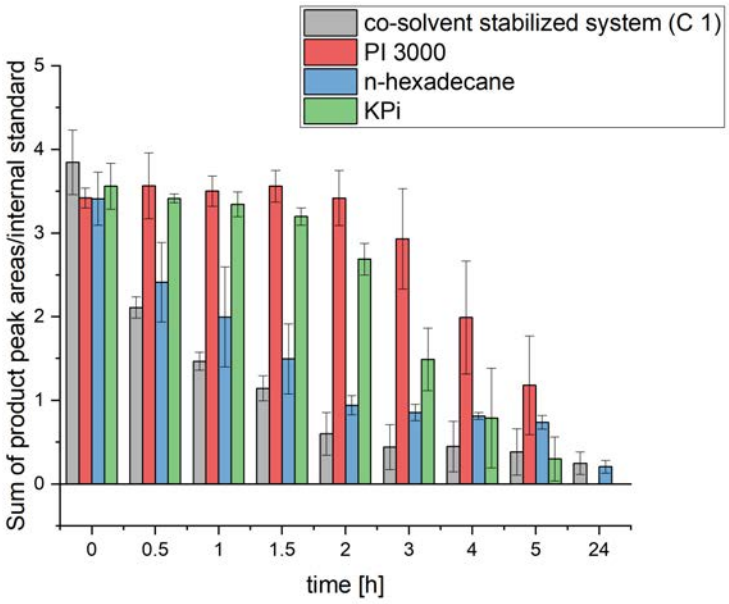

Figure S21. Enzyme degradation capability tracking over 24 hours. Co-solvent stabilized system (C 1) (grey), polyisoprene PI 3000 (red), *n*-hexadecane (blue) and potassium phosphate buffer (KPi) (green). Triplicates to determine the standard deviation.

Lcp_{K30} showed the longest residual activity for the co-solvent stabilized system (C 1) and the negative control of *n*-hexadecane in KPi 5 mM buffer. It is noteworthy that even though the enzyme's deactivation seems to be higher in the co-solvent stabilized system (C 1), it still leads to an increase in the area of integration (Table 3) for C 1 in comparison to N 1 (PI 3000). This shows the significant effect that emulsification has on the enzymatic degradation.

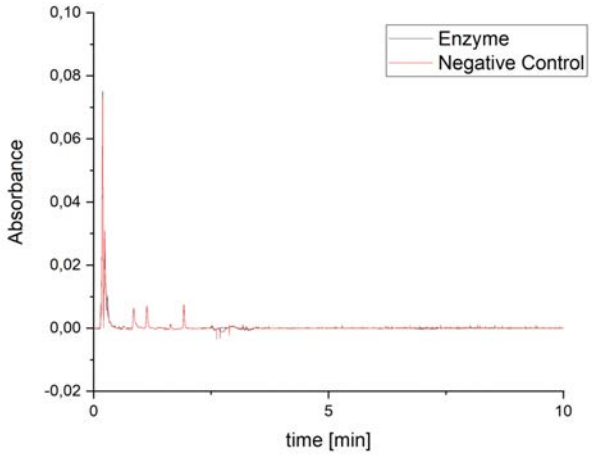

Figure S22. Stacked, baseline corrected UHPLC-curves of ethyl acetate extracts of a blind run with solely Lcp_{K30} enzyme (black) and the corresponding negative control (red).
This proves that the area of integration does not arise from the enzyme Lcp_{K30} itself.

5. Characterization data of the degradation products

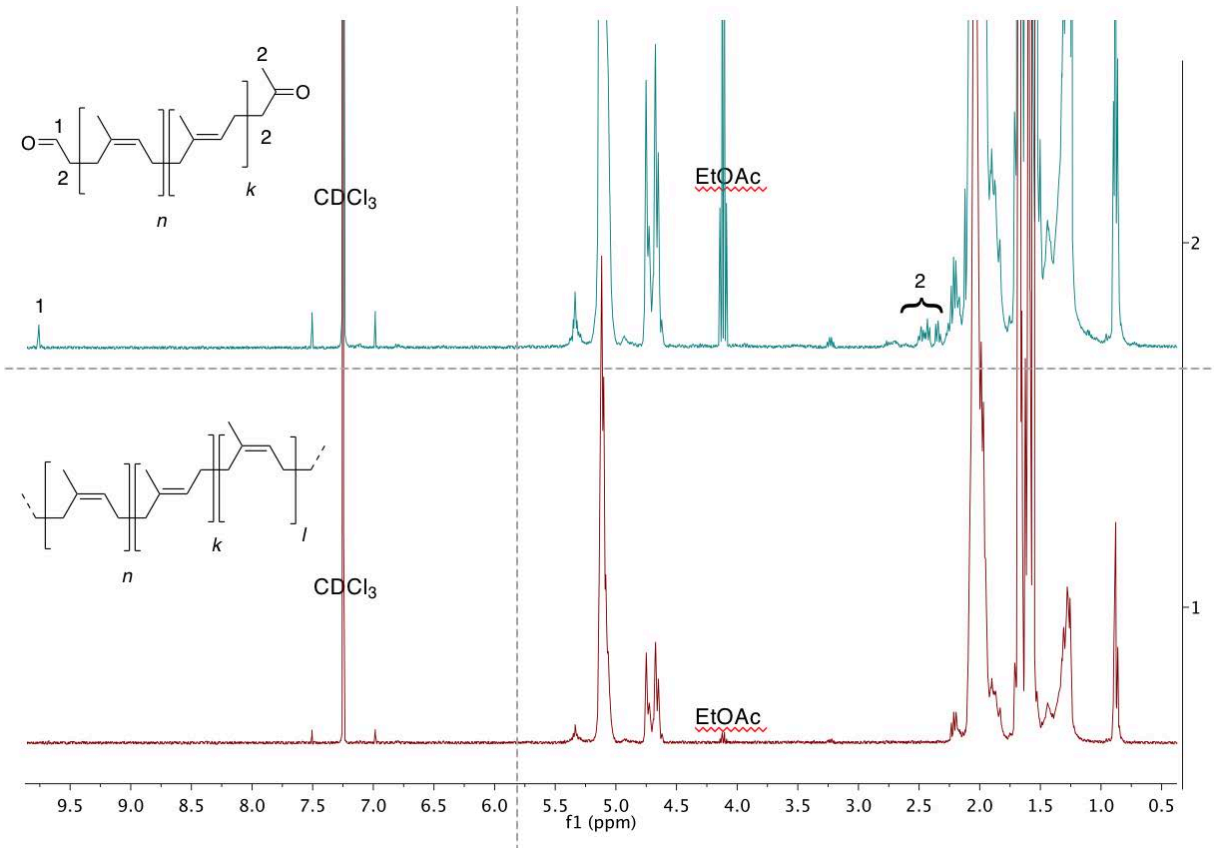

Figure S23. Stacked ^{1}H NMR of degraded and extracted non-emulsified PI 3000 (N 1, blue) and the respective negative control without enzyme (red).

Microstructure of 1 and 2 is reported in literature. [6-8]

Table S1. Oligo-isoprenoids generated by enzymatic cleavage of latex milk by Lcp_{K30}[5]

Elemental formula	$[M+H]^+$	*m/z* $[M+Na+CH_3OH]^+$
$C_{15}H_{24}O_2$	237.19	291.19
$C_{20}H_{32}O_2$	305.25	359.26
$C_{25}H_{40}O_2$	373.31	427.32
$C_{30}H_{48}O_2$	441.37	495.38
$C_{35}H_{56}O_2$	509.43	563.44
$C_{40}H_{64}O_2$	577.50	631.50
$C_{45}H_{72}O_2$	645.56	699.57
$C_{50}H_{80}O_2$	713.62	767.63
$C_{55}H_{88}O_2$	781.69	835.69
$C_{60}H_{96}O_2$	849.74	903.76
$C_{65}H_{104}O_2$	917.81	971.82

Table S2. Degradation fragments generated by enzymatic cleavage of reference latex milk (L 1) by Lcp_{K30} according to UHPLC-ESI-HRMS (Orbitrap) in positive ion mode

RT (min)	$[M+H]^+$ measured	$[M+H]^+$ calculated	Error (ppm)	Elemental Composition	RDBE
0.40	169.1224	169.1223	0.4	$C_{10}H_{17}O_2^+$	2.5
0.89	237.1849	237.1849	-0.1	$C_{15}H_{25}O_2^+$	3.5
3.24	305.2473	305.2475	-0.6	$C_{20}H_{33}O_2^+$	4.5
6.22	373.3095	373.3101	-1.7	$C_{25}H_{41}O_2^+$	5.5
7.06	441.3719	441.3727	-1.9	$C_{30}H_{49}O_2^+$	6.5
7.57	509.4343	509.4353	-2.0	$C_{35}H_{57}O_2^+$	7.5
8.01	577.4968	577.4979	-2.0	$C_{40}H_{65}O_2^+$	8.5
8.36	645.5595	645.5605	-1.5	$C_{45}H_{73}O_2^+$	9.5
8.69	713.6221	713.6231	-1.5	$C_{50}H_{81}O_2^+$	10.5
9.04	781.6844	781.6857	-1.6	$C_{55}H_{89}O_2^+$	11.5
9.45	849.7476	849.7483	-0.8	$C_{60}H_{97}O_2^+$	12.5
9.94	917.8108	917.8109	-0.1	$C_{65}H_{105}O_2^+$	13.5
10.60	985.8728	985.8735	-0.7	$C_{70}H_{113}O_2^+$	14.5

Table S3. Degradation fragments generated by enzymatic cleavage of co-solvent emulsified synthetic polyisoprene (C 1) by Lcp_{K30} according to UHPLC-ESI-HRMS (Orbitrap) in positive ion mode

RT (min)	$[M+H]^+$ measured	$[M+H]^+$ calculated	Error (ppm)	Elemental Composition	RDBE
0.43	169.1224	169.1223	0.3	$C_{10}H_{17}O_2^+$	2.5
0.88	237.1850	237.1849	0.2	$C_{15}H_{25}O_2^+$	3.5
3.30	305.2475	305.2475	-0.5	$C_{20}H_{33}O_2^+$	4.5
6.23	373.3096	373.3101	-1.4	$C_{25}H_{41}O_2^+$	5.5
7.01	441.3725	441.3727	-0.4	$C_{30}H_{49}O_2^+$	6.5
7.61	509.4346	509.4353	-1.5	$C_{35}H_{57}O_2^+$	7.5
7.99	577.4969	577.4979	-1.7	$C_{40}H_{65}O_2^+$	8.5
8.39	645.5595	645.5605	-1.5	$C_{45}H_{73}O_2^+$	9.5
8.66	713.6230	713.6231	-0.2	$C_{50}H_{81}O_2^+$	10.5
9.03	781.6857	781.6857	-0.1	$C_{55}H_{89}O_2^+$	11.5
9.45	849.7474	849.7483	-1.1	$C_{60}H_{97}O_2^+$	12.5
9.94	917.8104	917.8109	-0.5	$C_{65}H_{105}O_2^+$	13.5
10.60	985.8733	985.8735	-0.2	$C_{70}H_{113}O_2^+$	14.5

Table S4. Degradation fragments generated by enzymatic cleavage of co-solvent emulsified synthetic polyisoprene (C 1) and of reference latex milk (L 1) by Lcp_{K30} according to UHPLC-UV-ESI-HRMS (QTOF) in positive ion mode

RT (min) L 1	RT (min) C 1	RT_{UV} (min) L 1	RT_{UV} (min) C 1	[M-H]+ measured L1	[M-H]+ measured C 1	[M-H]+ calculated	Error (ppm) Latex	Elemental Composition	RDBE
n.d	0.64	n.d.	0.58	-	169.1217	169.1223	-3.6, S	$C_{10}H_{17}O_2$	2.5
1.12	1.17	1.051	.1.02	237.1843	237.1852	237.1849	-2.6	$C_{15}H_{24}O_2$	3.5
2.57	2.59	2.54	2.55	305.2476	305.2475	305.2475	0.3	$C_{20}H_{32}O_2$	4.5
3.48	3.50	3.43	3.47	373.3103	373.3089	373.3101	0.5	$C_{25}H_{40}O_2$	5.5
4.02	4.03	3.98	3.97	441.3722	441.3714	441.3727	-1.2	$C_{30}H_{48}O_2$	6.5
4.40	4.40	4.36	4.39	509.4336	509.4350	509.4353	-3.4	$C_{35}H_{56}O_2$	7.5
4.67	4.65	4.65	4.72	577.4979	577.4968	577.4979	0.1	$C_{40}H_{64}O_2$	8.5
4.93	4.94	4.90	5.02	645.5621	645.5593	645.5605	2.5	$C_{45}H_{73}O_2$	9.5
5.17	5.15	5.13	5.29	713.6221	713.6212	713.6231	0.8	$C_{50}H_{80}O_2$	10.5
5.46	5.44	5.42	5.64	781.6848	781.6828	781.6857	-1.2	$C_{55}H_{88}O_2$	11.5
5.83	5.80	5.78	5.81	849.7466	849.7463	849.7483	-2.0	$C_{60}H_{96}O_2$	12.5
6.32	n.d.	6.28	n.d.	917.8092	n.d.	917.8109	-1.9	$C_{65}H_{104}O_2$	13.5
7.04	n.d.	6.96	n.d.	985.8713	n.d.	985.8735	-2.2	$C_{70}H_{112}O_2$	14.5
8.05	n.d.	7.98	n.d.	1053.9330	n.d.	1053.9361	-3.0	$C_{75}H_{120}O_2$	15.5
9.18	n.d.	9.21	n.d.	1121.9984	n.d.	1121.9987	-0.3	$C_{80}H_{129}O_2$	16.5
n.d.	n.d.	10.95	n.d.	n.d.	n.d.	1191	n.d.	$C_{85}H_{137}O_2$	n.d.

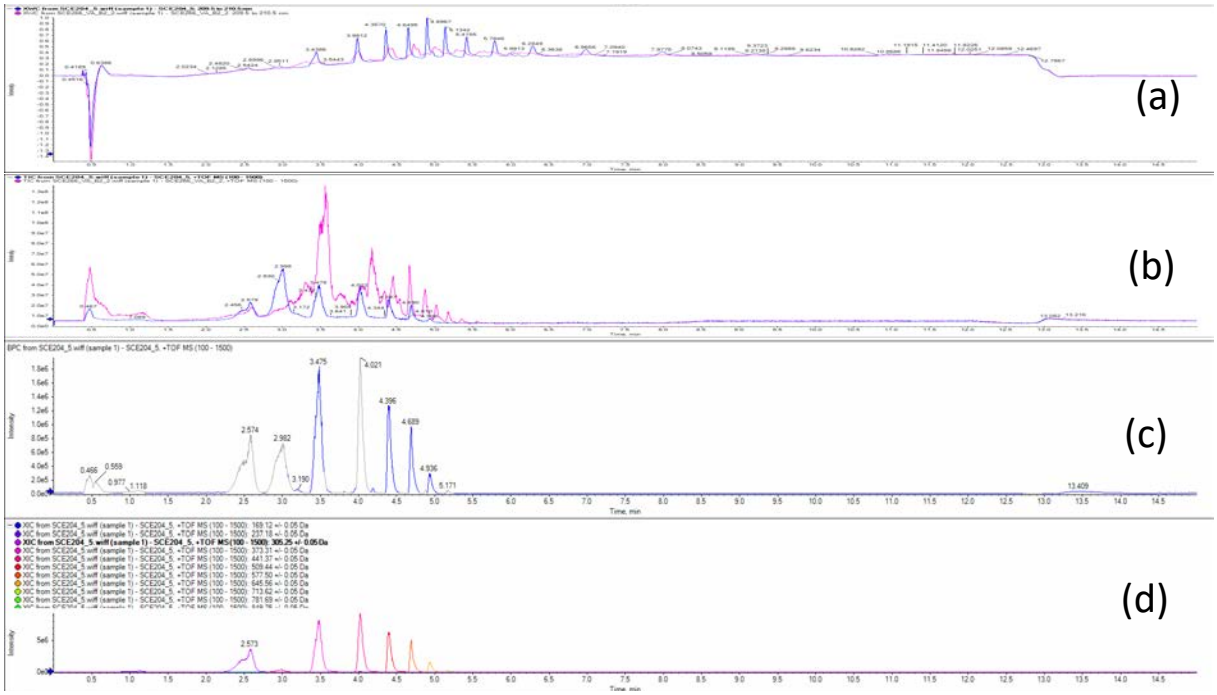

Figure S24. Stacked UV-curves (a) of enzymatically degraded L 1 (blue) and enzymatically degraded C 1 (pink), stacked total ion chromatograms (TIC) (b) of enzymatically degraded L 1 (blue) and enzymatically degraded C 1 (pink) and extracted ion chromatograms (EICs) of enzymatically degraded L 1 (c) and enzymatically degraded C 1 (d) acquired during UHPLC-UV-ESI-HRMS measurement.

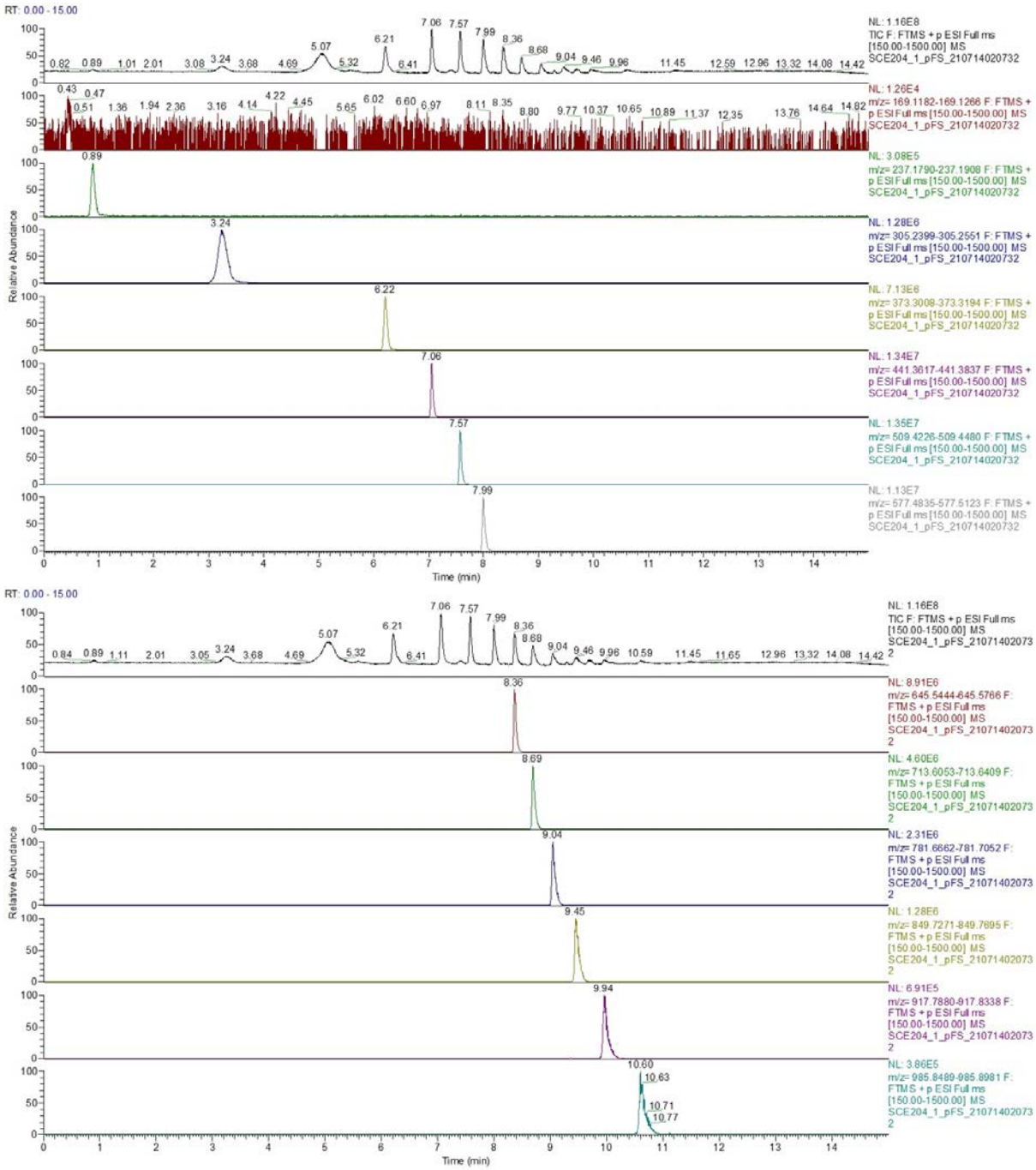

Figure S25. Total ion chromatogram (TIC) and extracted ion chromatograms (EICs) of enzymatically degraded L 1 acquired during UHPLC-ESI-HRMS measurement.

For the data evaluation, the target *m/z* values were extracted from the TIC using a 25 ppm mass window with a mass accuracy of four decimals to obtain the corresponding EIC for each analyte according to the degradation patterns seen in literature. [5]

.

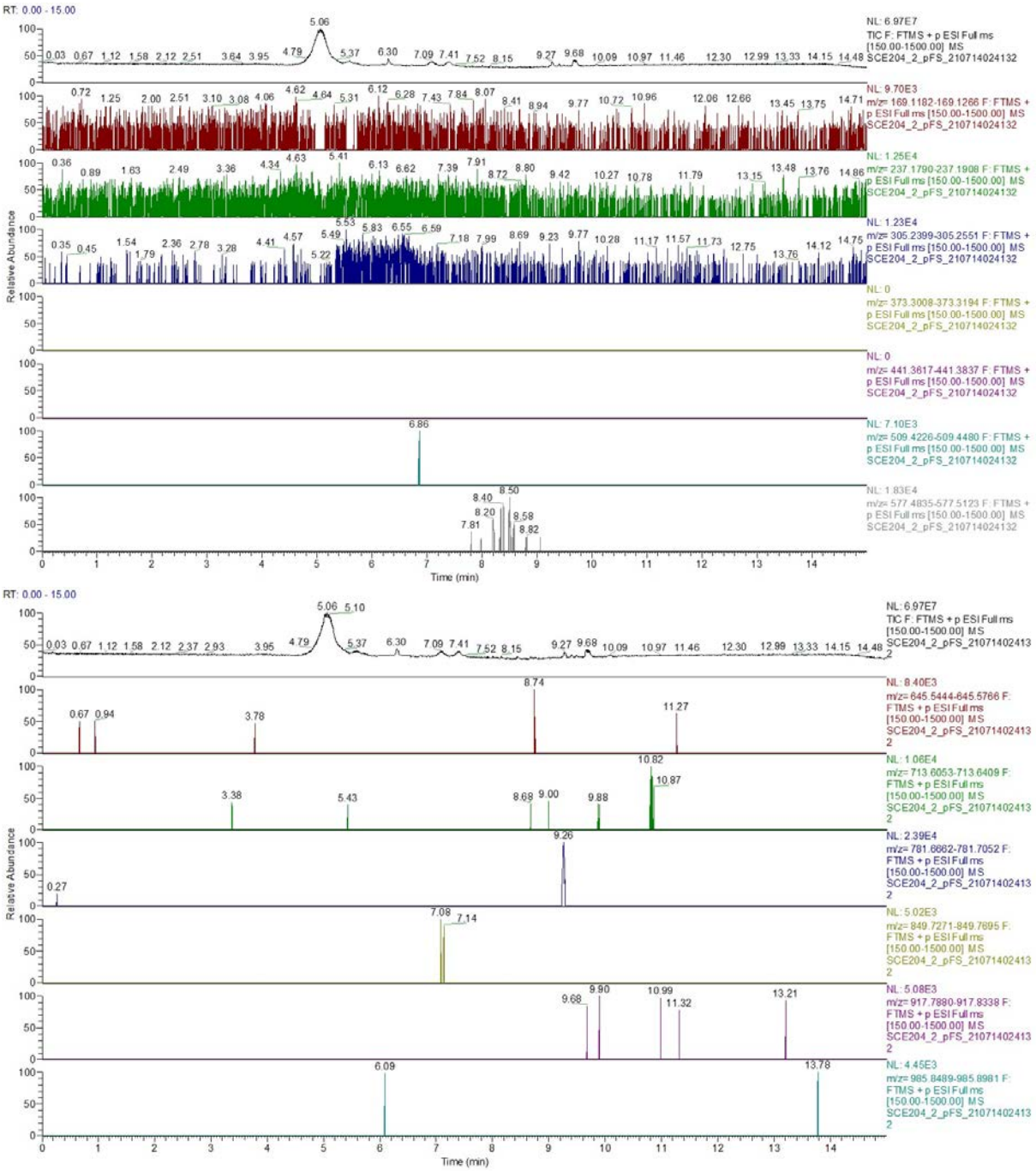

Figure S26. Total ion chromatogram (TIC) and extracted ion chromatograms (EICs) of the negative control of L 1 acquired during UHPLC-ESI-HRMS measurement.

For the data evaluation, the target *m/z* values were extracted from the TIC using a 25 ppm mass window with a mass accuracy of four decimals to obtain the corresponding EIC for each analyte according to the degradation patterns seen in literature. [5]

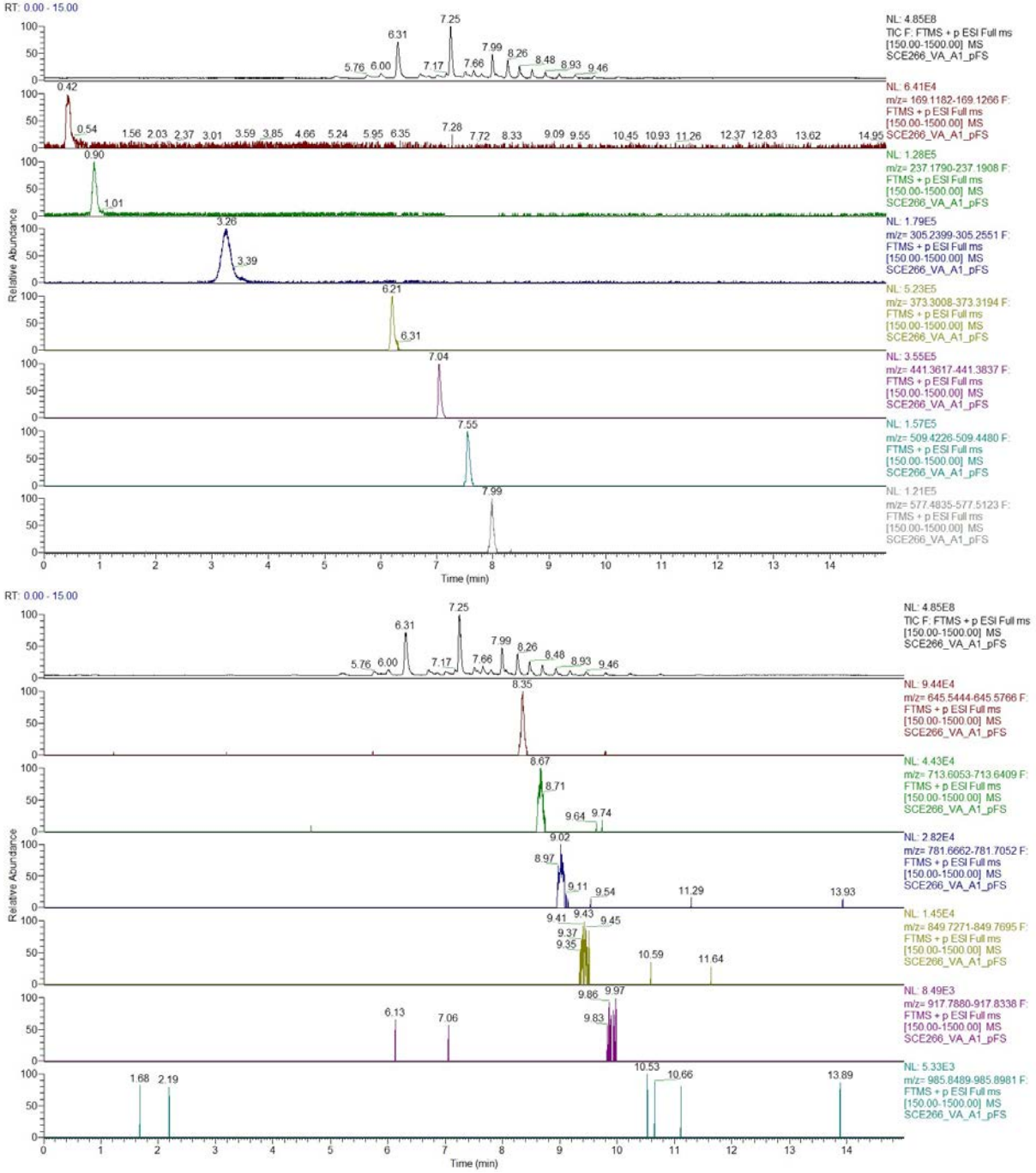

Figure S27. Total ion chromatogram (TIC) and extracted ion chromatograms (EICs) of enzymatically degraded N 1 acquired during UHPLC-ESI-HRMS measurement.

For the data evaluation, the target *m/z* values were extracted from the TIC using a 25 ppm mass window with a mass accuracy of four decimals to obtain the corresponding EIC for each analyte according to the degradation patterns seen in literature. [5]

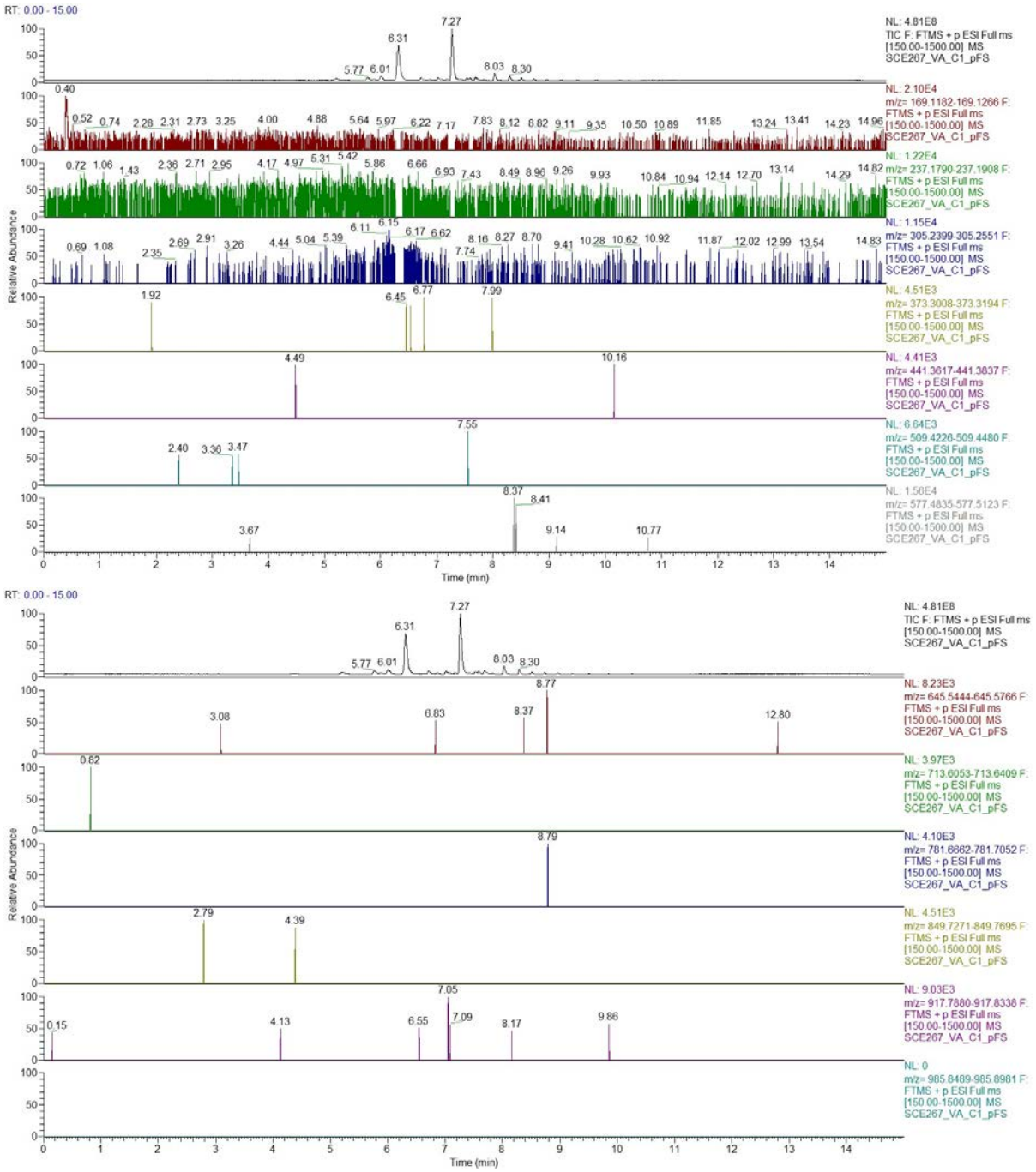

Figure S28. Total ion chromatogram (TIC) and extracted ion chromatograms (EICs) of the negative control of N 1 acquired during UHPLC-ESI-HRMS measurement.

For the data evaluation, the target *m/z* values were extracted from the TIC using a 25 ppm mass window with a mass accuracy of four decimals to obtain the corresponding EIC for each analyte according to the degradation patterns seen in literature. [5]

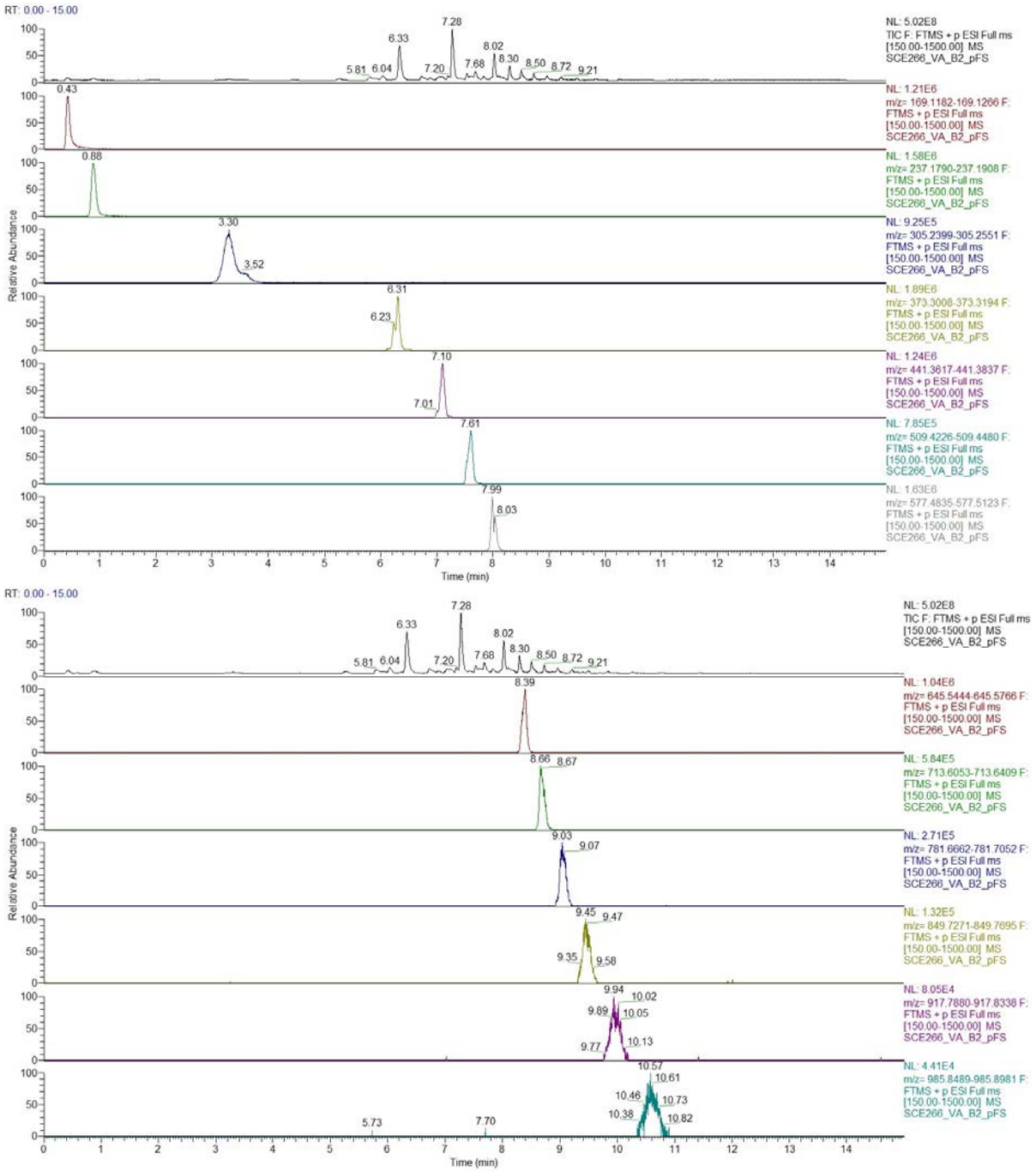

Figure S29. Total ion chromatogram (TIC) and extracted ion chromatograms (EICs) of enzymatically degraded C 1 acquired during UHPLC-ESI-HRMS measurement.

For the data evaluation, the target *m/z* values were extracted from the TIC using a 25 ppm mass window with a mass accuracy of four decimals to obtain the corresponding EIC for each analyte according to the degradation patterns seen in literature. [5]

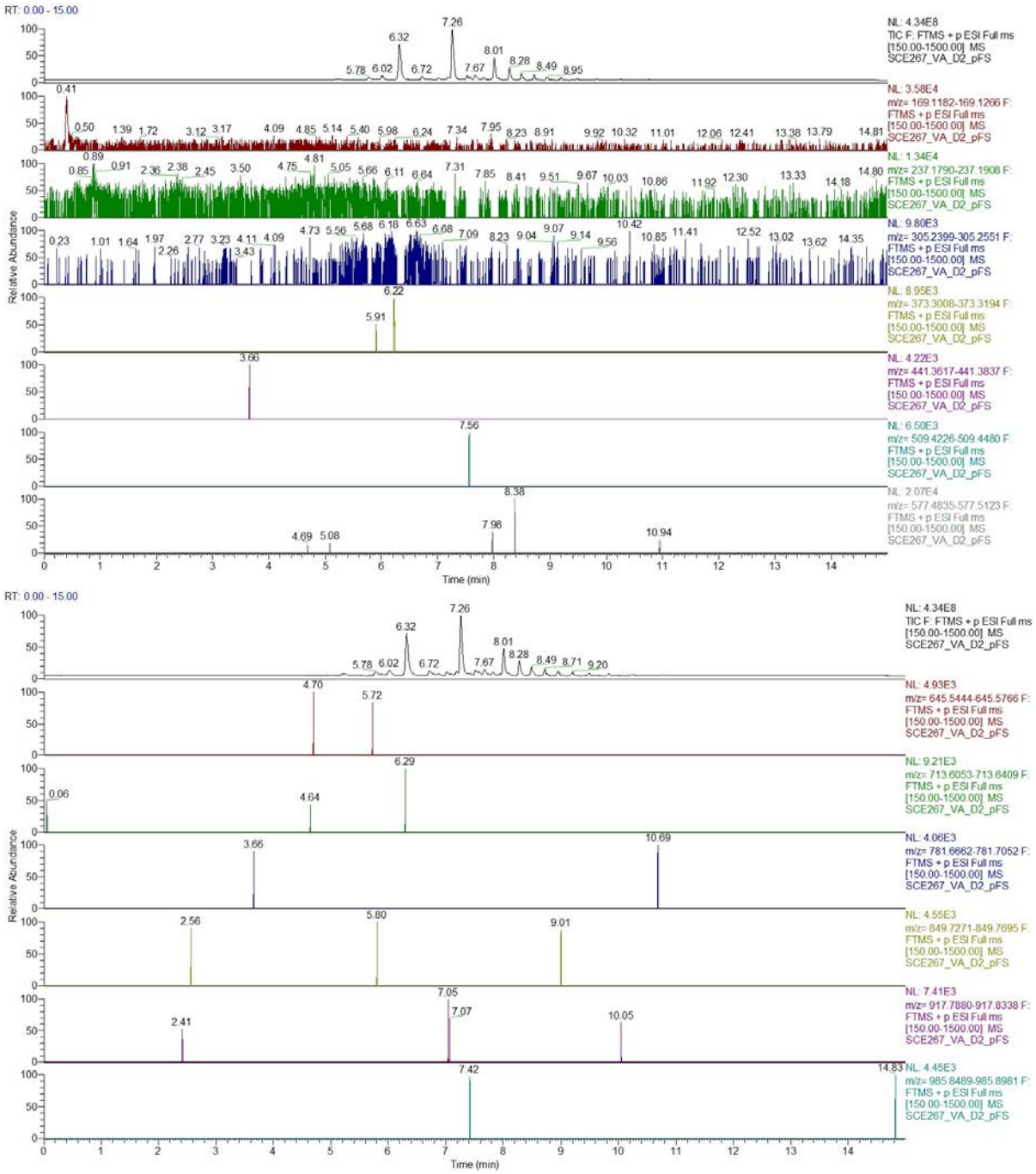

Figure S30. Total ion chromatogram (TIC) and extracted ion chromatograms (EICs) of the negative control of C 1 acquired during UHPLC-ESI-HRMS measurement.

For the data evaluation, the target *m/z* values were extracted from the TIC using a 25 ppm mass window with a mass accuracy of four decimals to obtain the corresponding EIC for each analyte according to the degradation patterns seen in literature. [5]

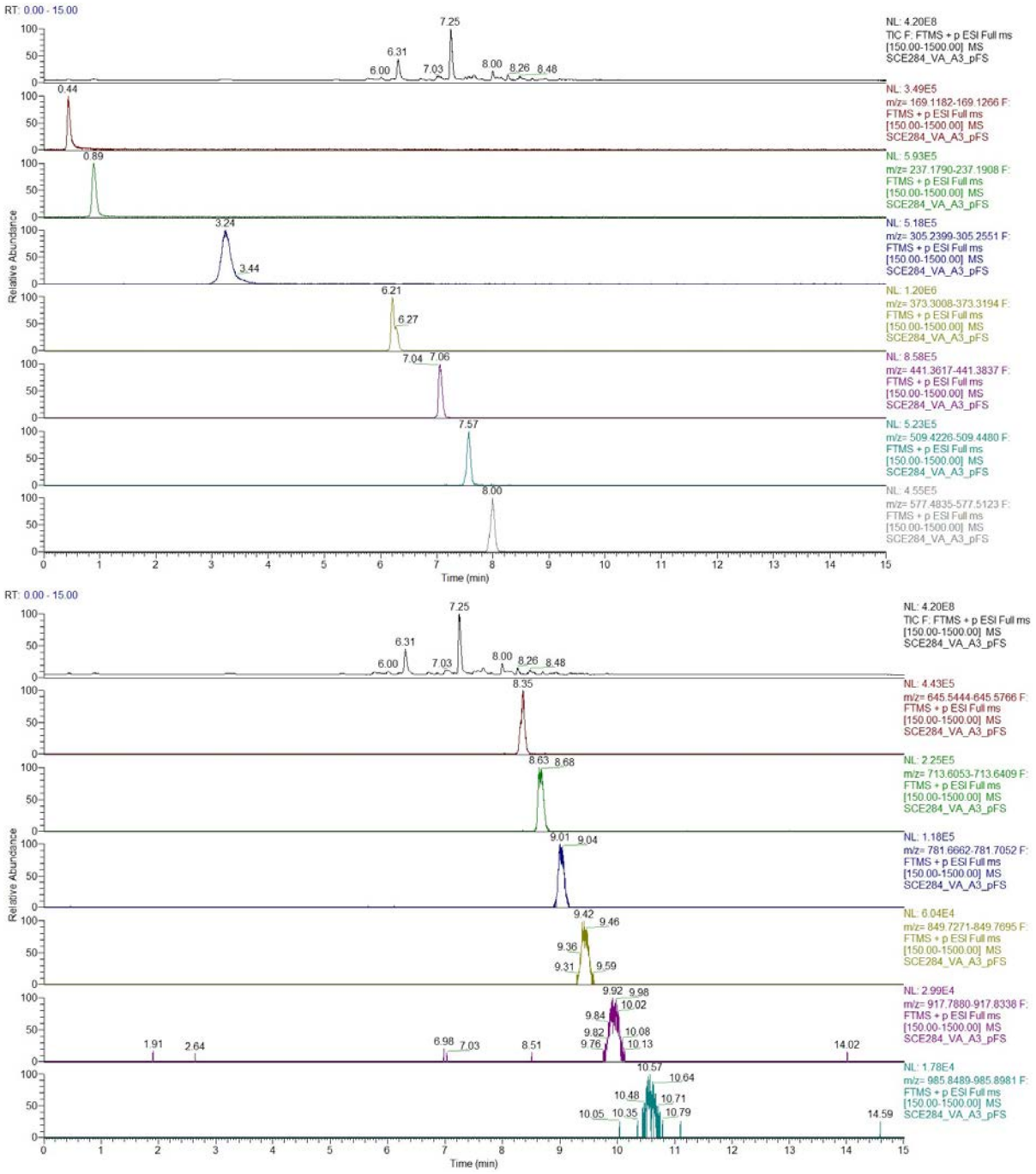

Figure S31. Total ion chromatogram (TIC) and extracted ion chromatograms (EICs) of enzymatically degraded A 1 acquired during UHPLC-ESI-HRMS measurement.

For the data evaluation, the target *m/z* values were extracted from the TIC using a 25 ppm mass window with a mass accuracy of four decimals to obtain the corresponding EIC for each analyte according to the degradation patterns seen in literature. [5]

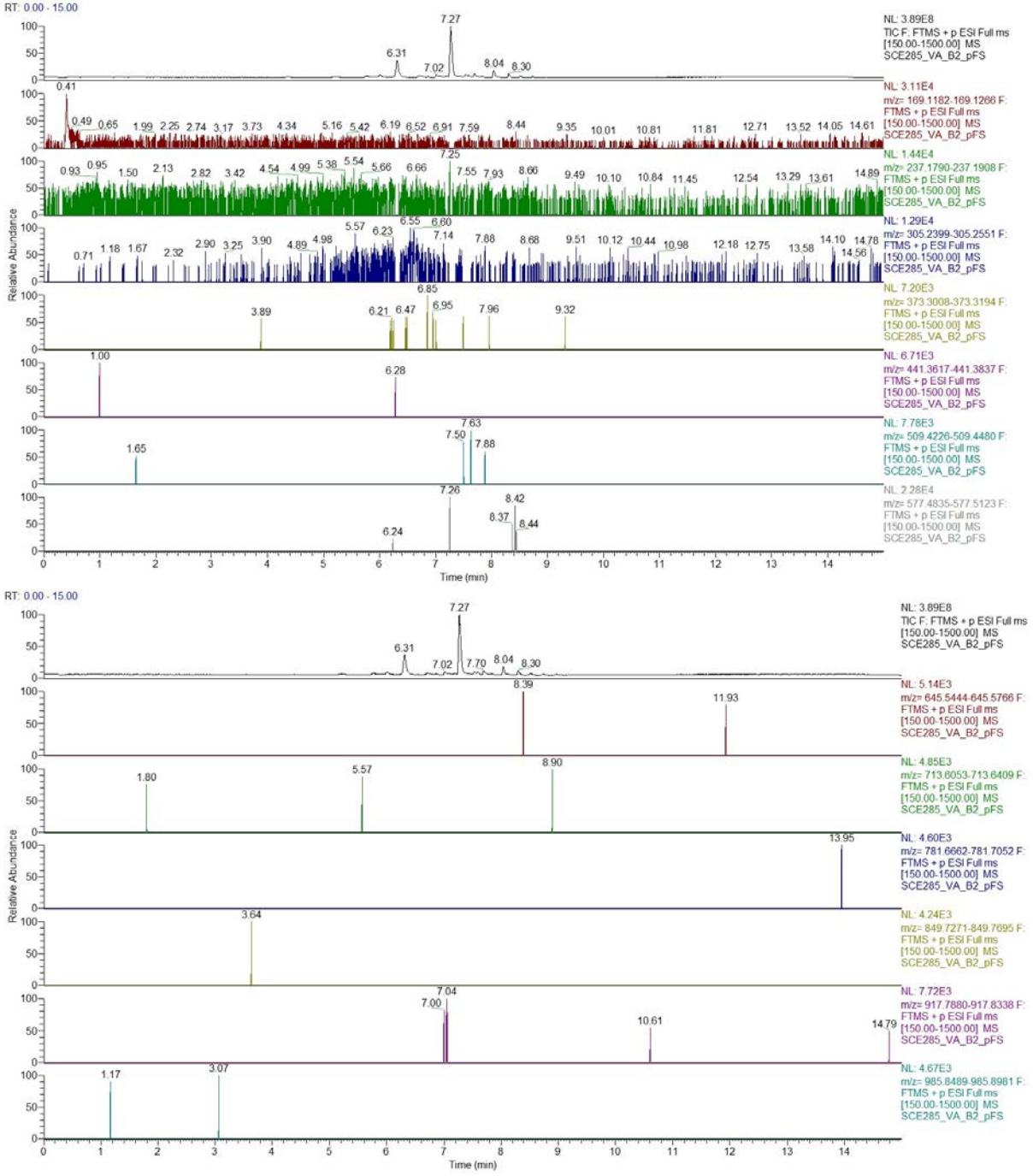

Figure S32. Total ion chromatogram (TIC) and extracted ion chromatograms (EICs) of the negative control of A 1 acquired during UHPLC-ESI-HRMS measurement.

For the data evaluation, the target *m/z* values were extracted from the TIC using a 25 ppm mass window with a mass accuracy of four decimals to obtain the corresponding EIC for each analyte according to the degradation patterns seen in literature. [5]

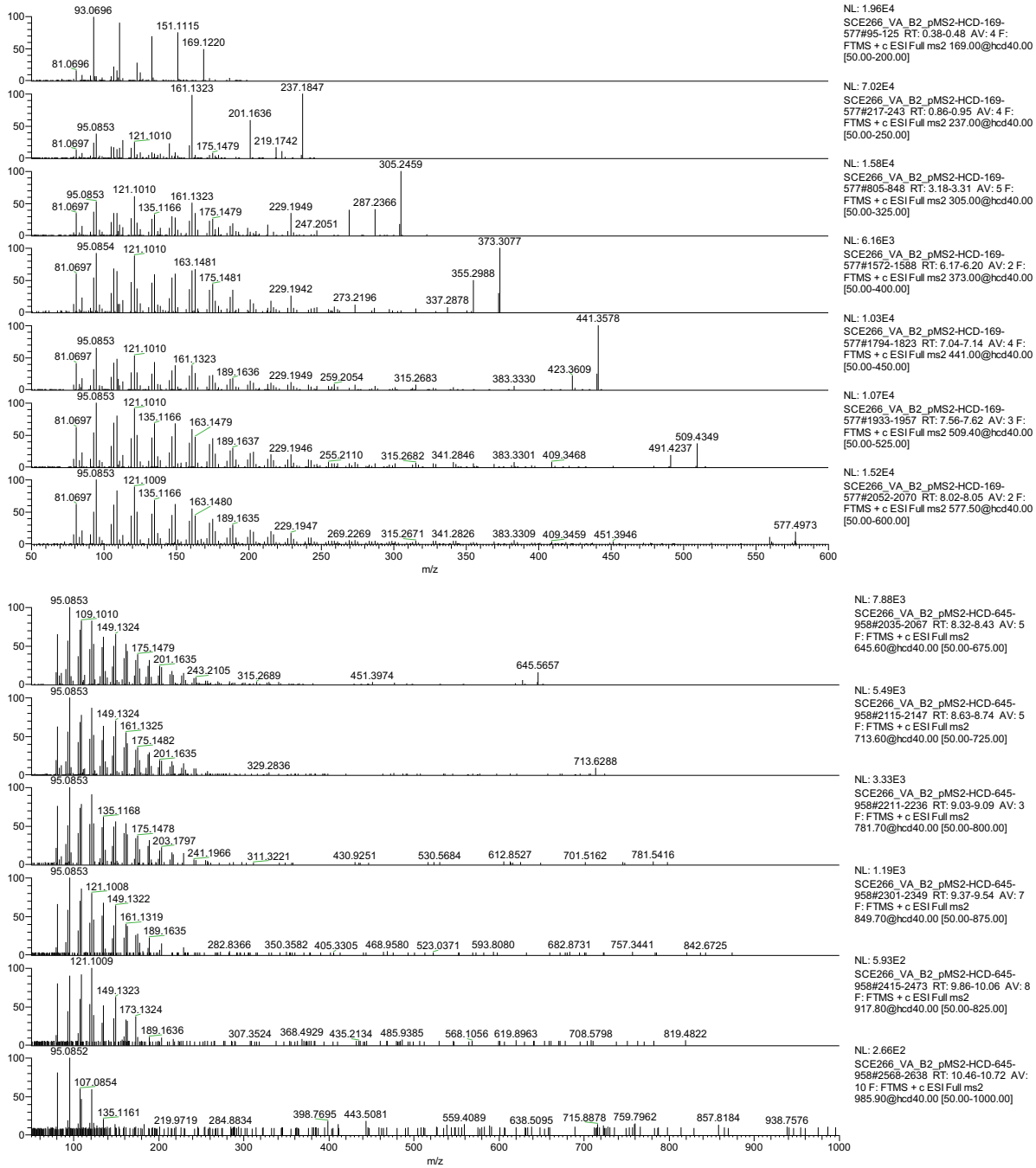

Figure S33. Comparison of the positive ion UHPLC-ESI-HRMS/MS spectra of the detected degradation products of synthetic polyisoprene C1.

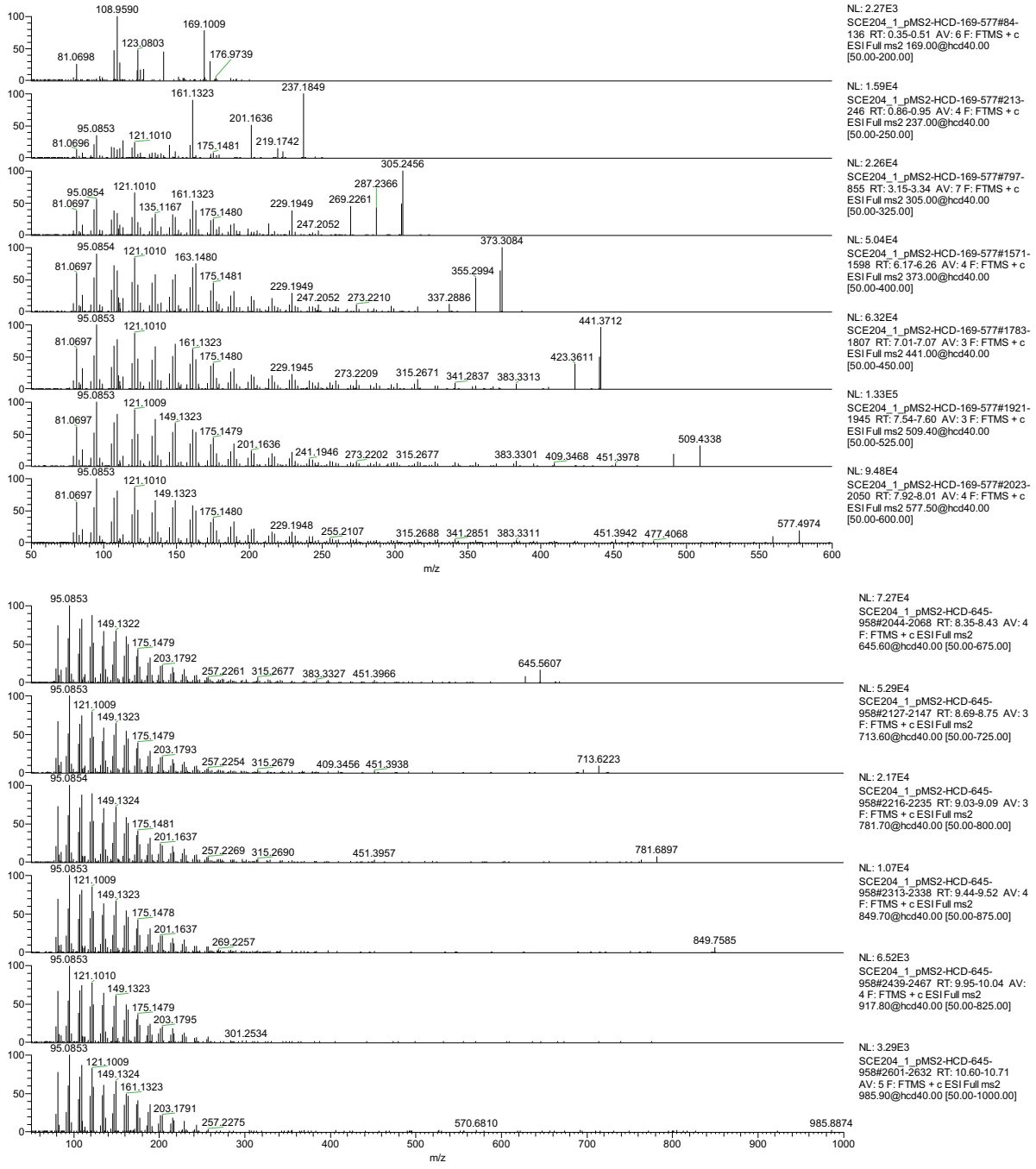

Figure S34. Comparison of the positive ion UHPLC-ESI-HRMS/MS spectra of the detected degradation products of natural polyisoprene L1.

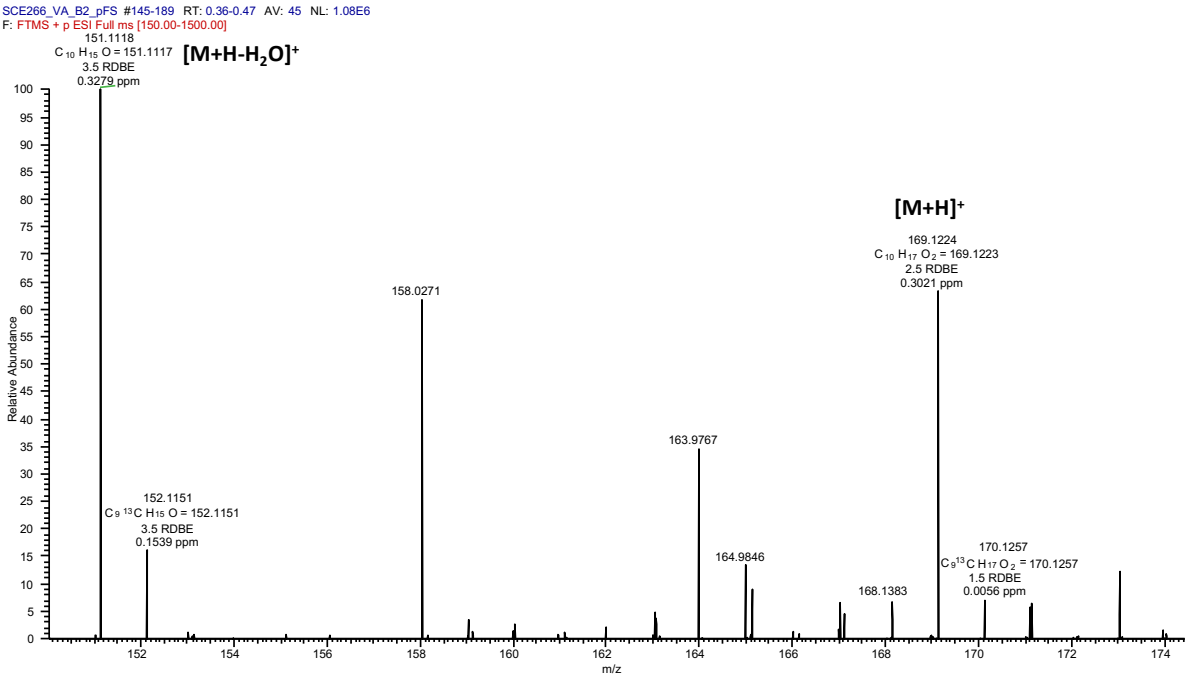

Figure S35. (+)-ESI-HRMS spectrum of the degradation fragments with elemental composition of $C_{10}H_{16}O_2$. obtained from C1.

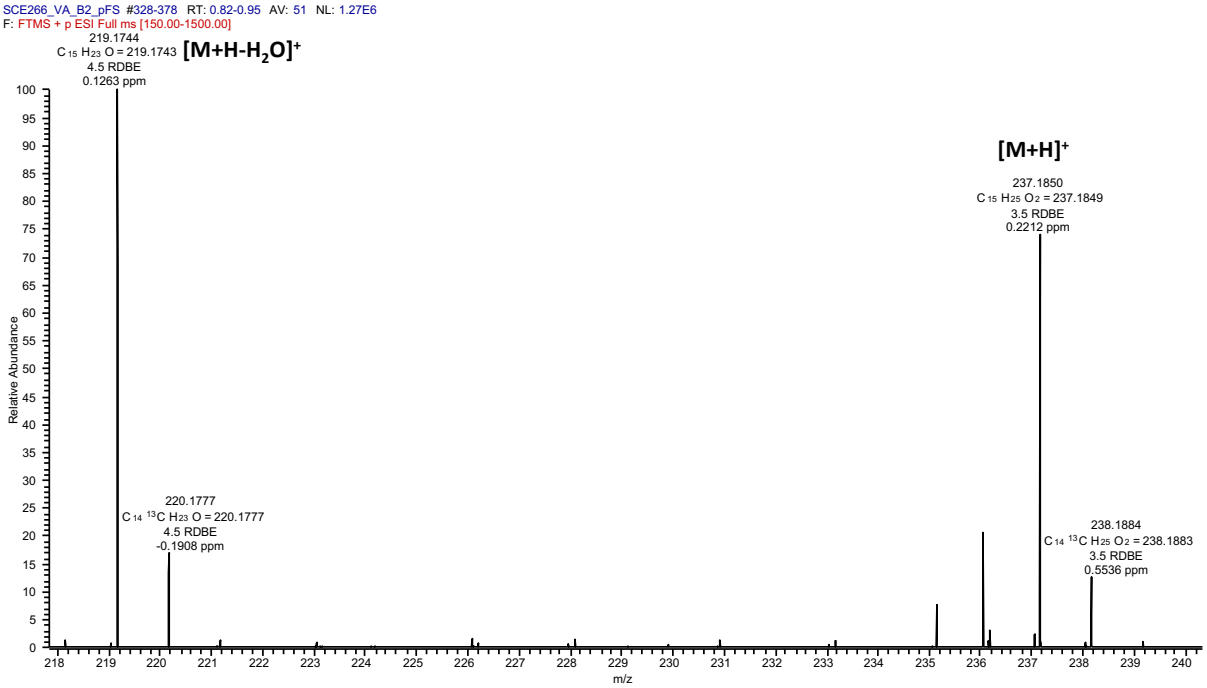

Figure S36. (+)-ESI-HRMS spectrum of the degradation fragments with elemental composition of $C_{15}H_{24}O_2$ obtained from C1.

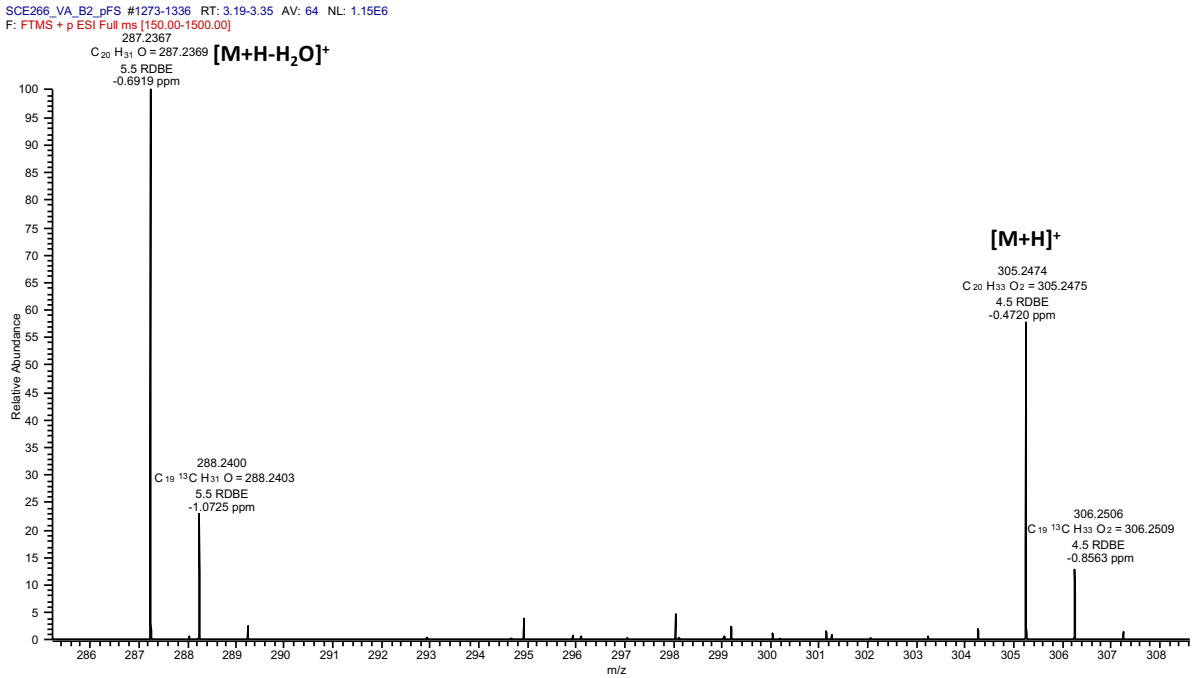

Figure S37. (+)-ESI-HRMS spectrum of the degradation fragments with elemental composition of $C_{20}H_{32}O_2$ obtained from C1.

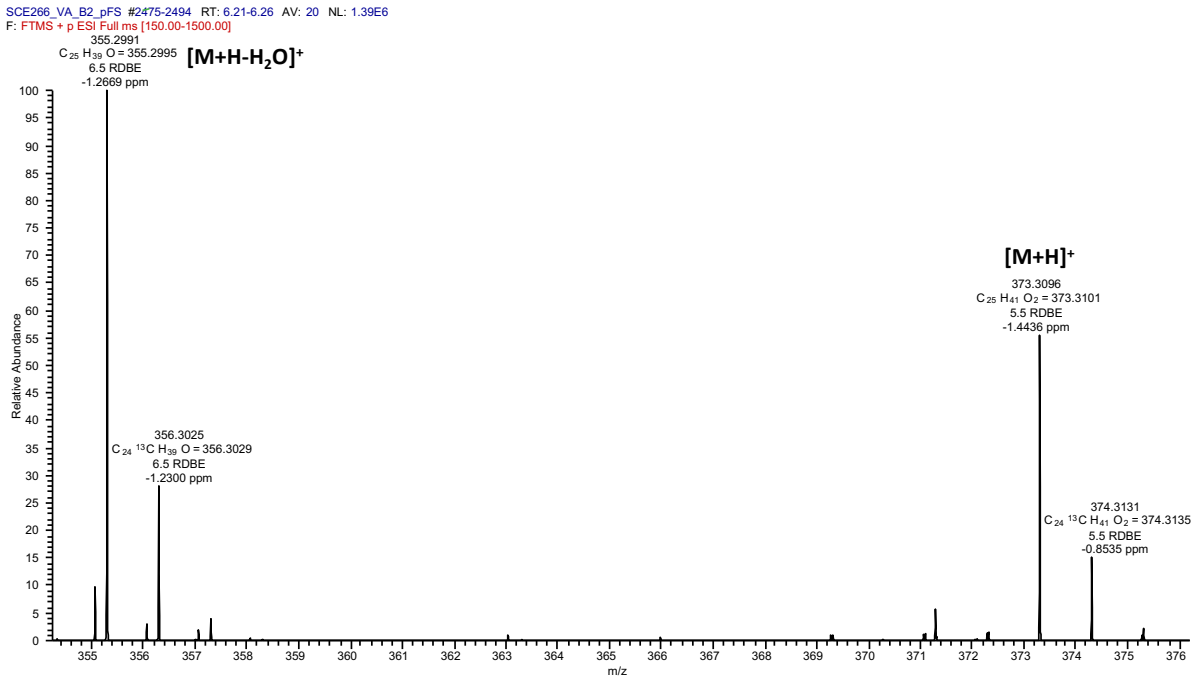

Figure S38. (+)-ESI-HRMS spectrum of the degradation fragments with elemental composition of $C_{25}H_{40}O_2$ obtained from C1.

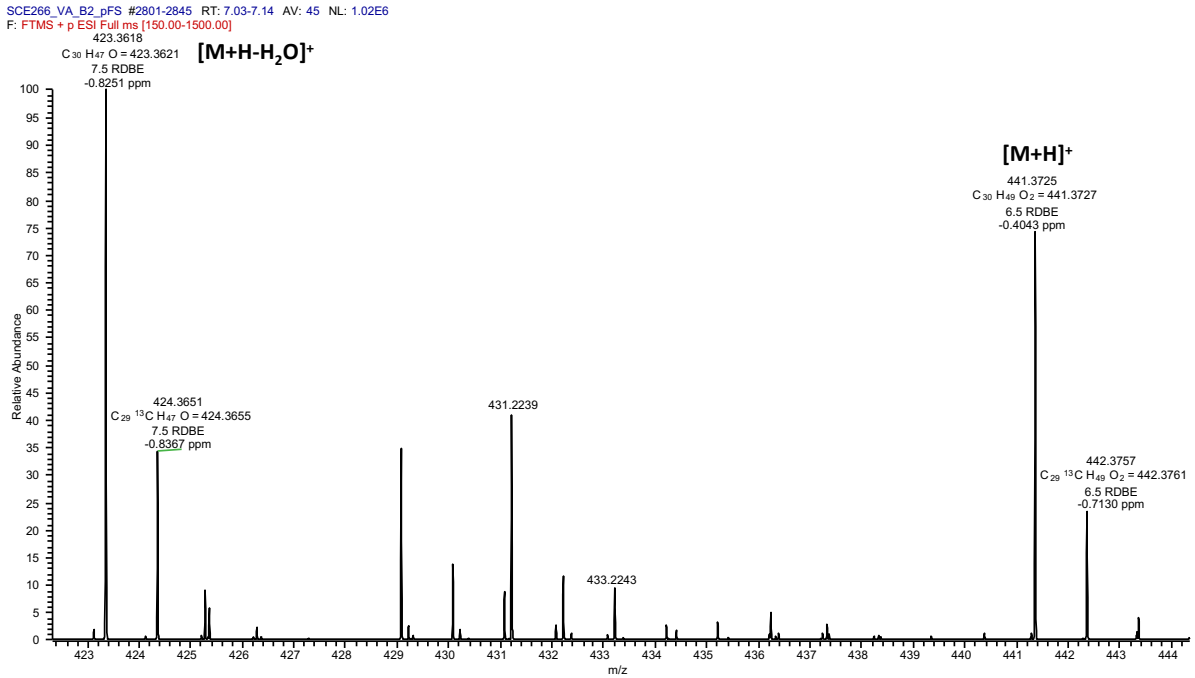

Figure S39. (+)-ESI-HRMS spectrum of the degradation fragments with elemental composition of $C_{30}H_{48}O_2$ obtained from C1.

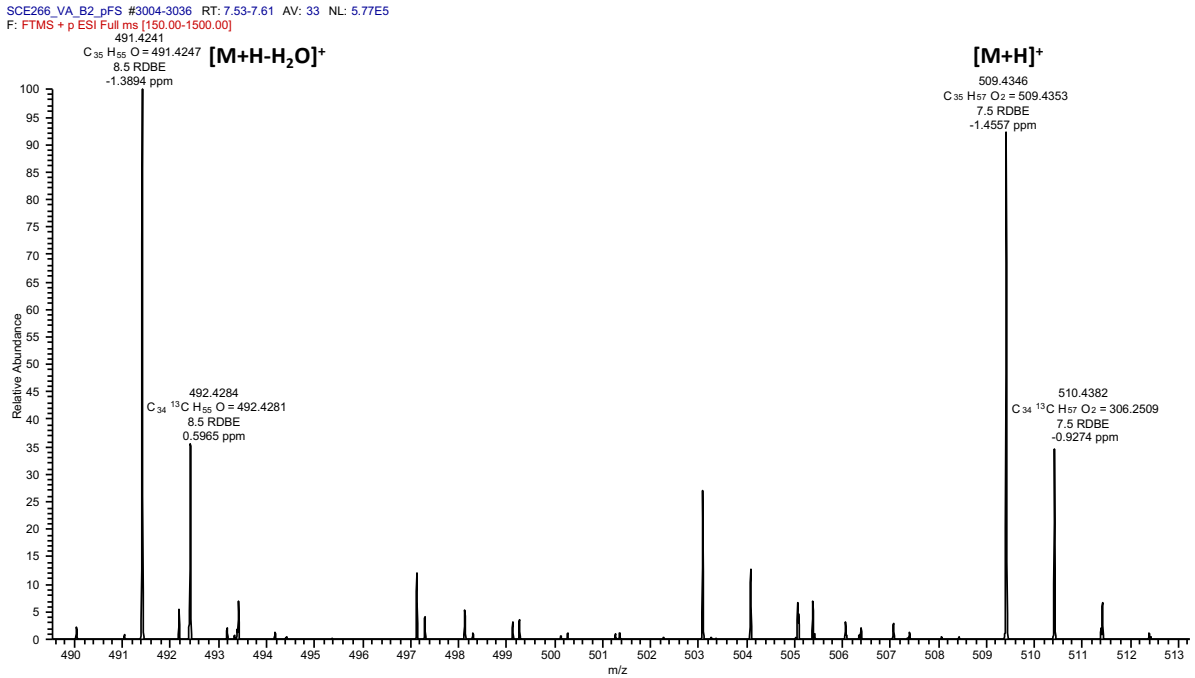

Figure S40. (+)-ESI-HRMS spectrum of the degradation fragments with elemental composition of $C_{35}H_{56}O_2$ obtained from C1.

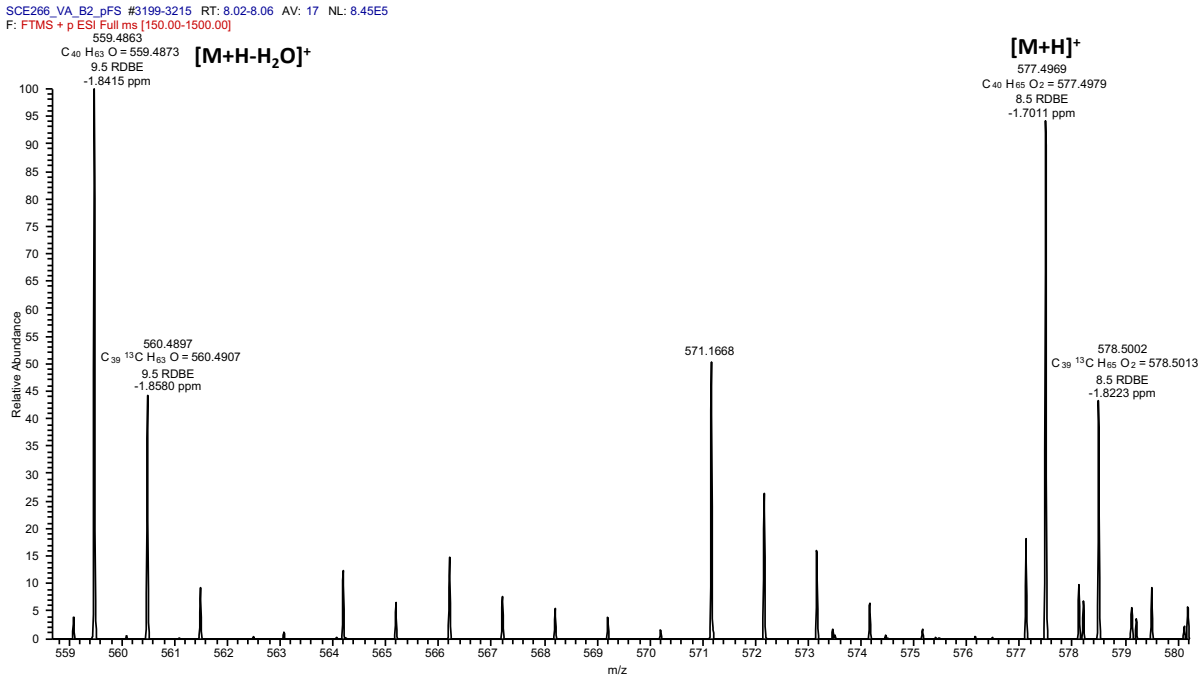

Figure S41. (+)-ESI-HRMS spectrum of the degradation fragments with elemental composition of $C_{40}H_{64}O_2$ obtained from C1.

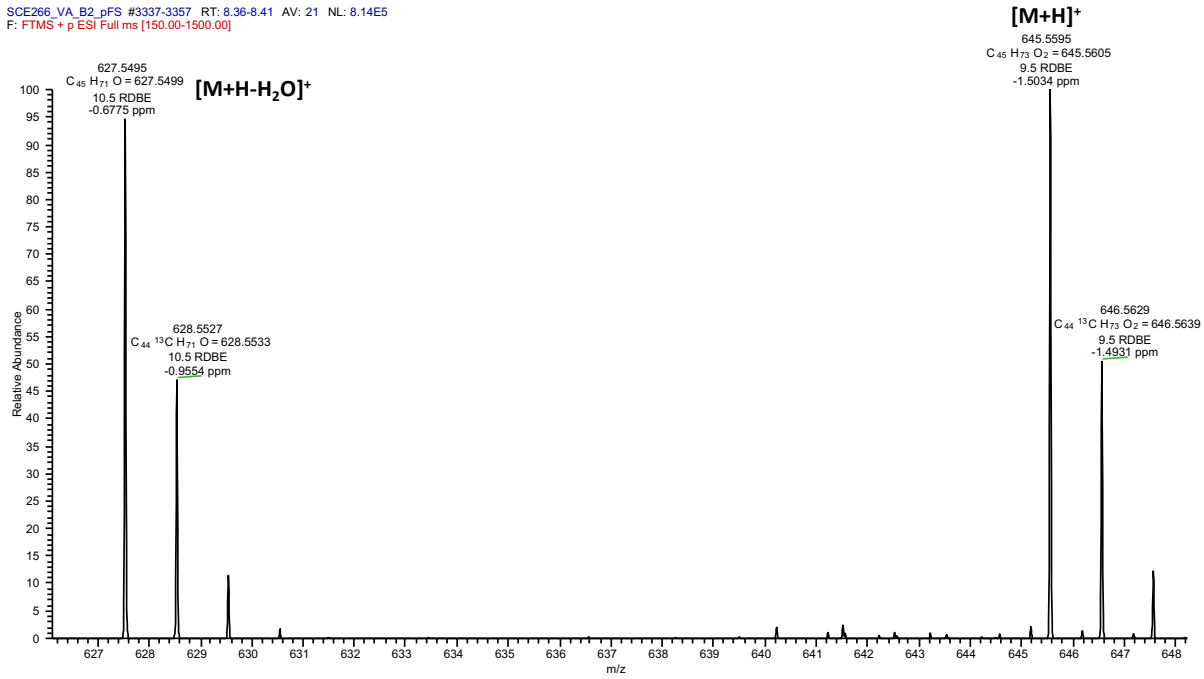

Figure S42. (+)-ESI-HRMS spectrum of the degradation fragments with elemental composition of $C_{45}H_{72}O_2$ obtained from C1.

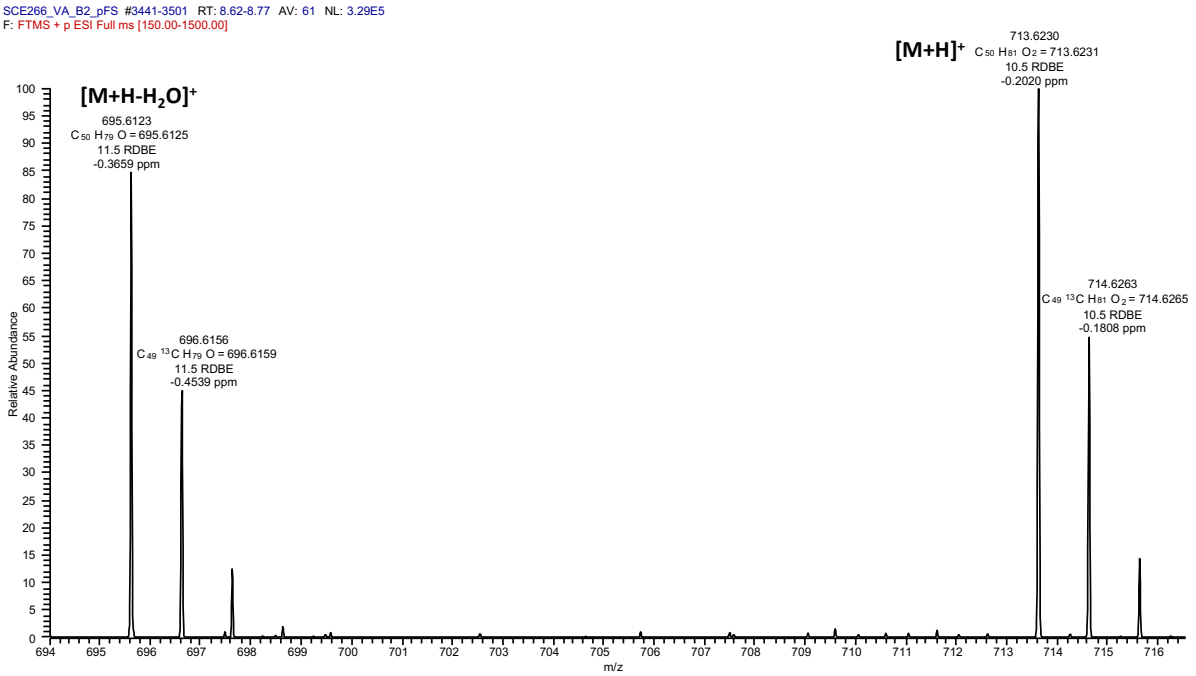

Figure S43. (+)-ESI-HRMS spectrum of the degradation fragments with elemental composition of $C_{50}H_{80}O_2$ obtained from C1.

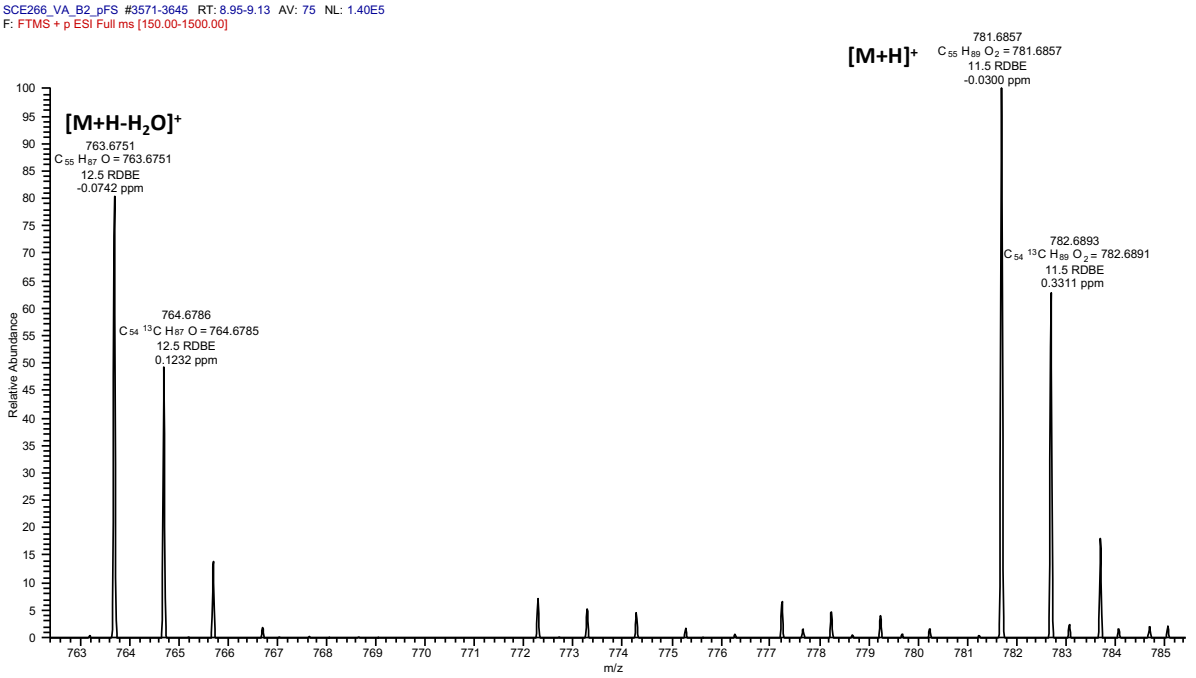

Figure S44. (+)-ESI-HRMS spectrum of the degradation fragments with elemental composition of $C_{55}H_{88}O_2$ obtained from C1.

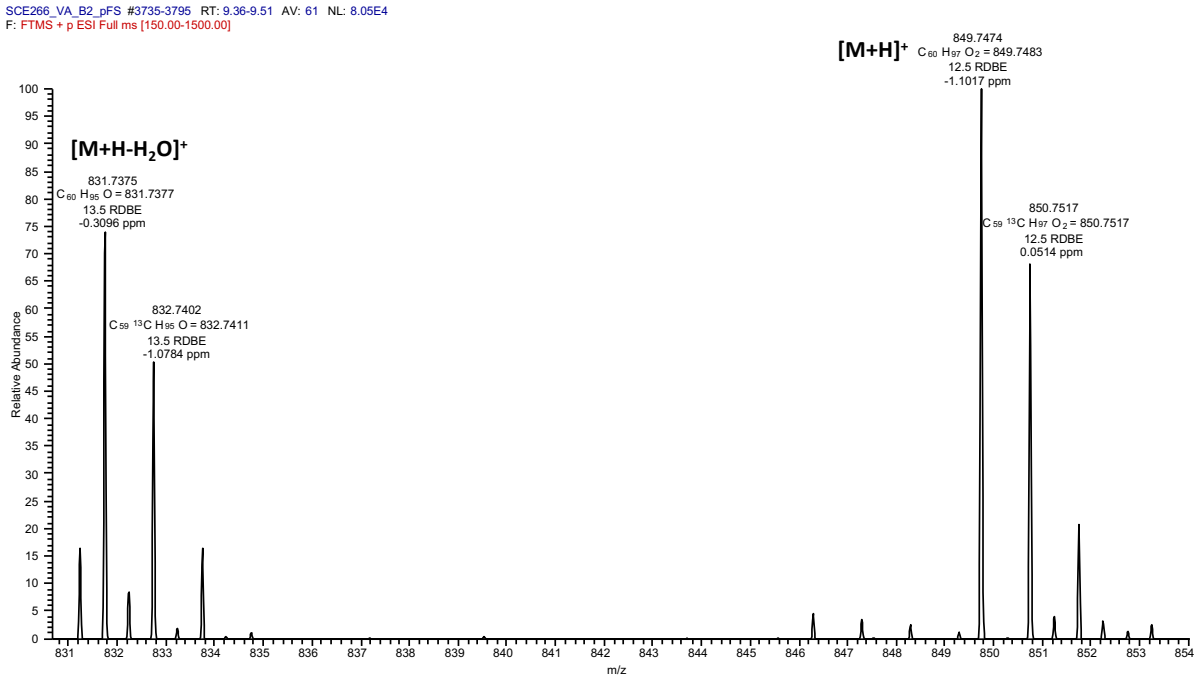

Figure S45. (+)-ESI-HRMS spectrum of the degradation fragments with elemental composition of $C_{60}H_{96}O_2$ obtained from C1.

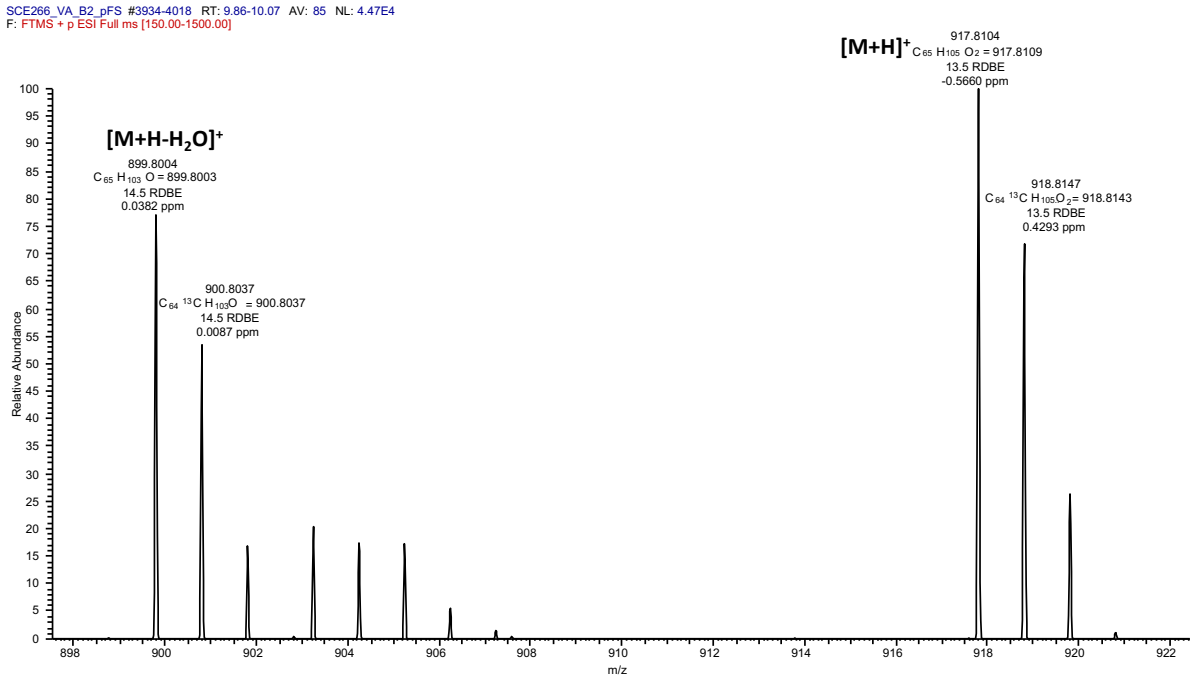

Figure S46. (+)-ESI-HRMS spectrum of the degradation fragments with elemental composition of $C_{65}H_{104}O_2$ obtained from C1.

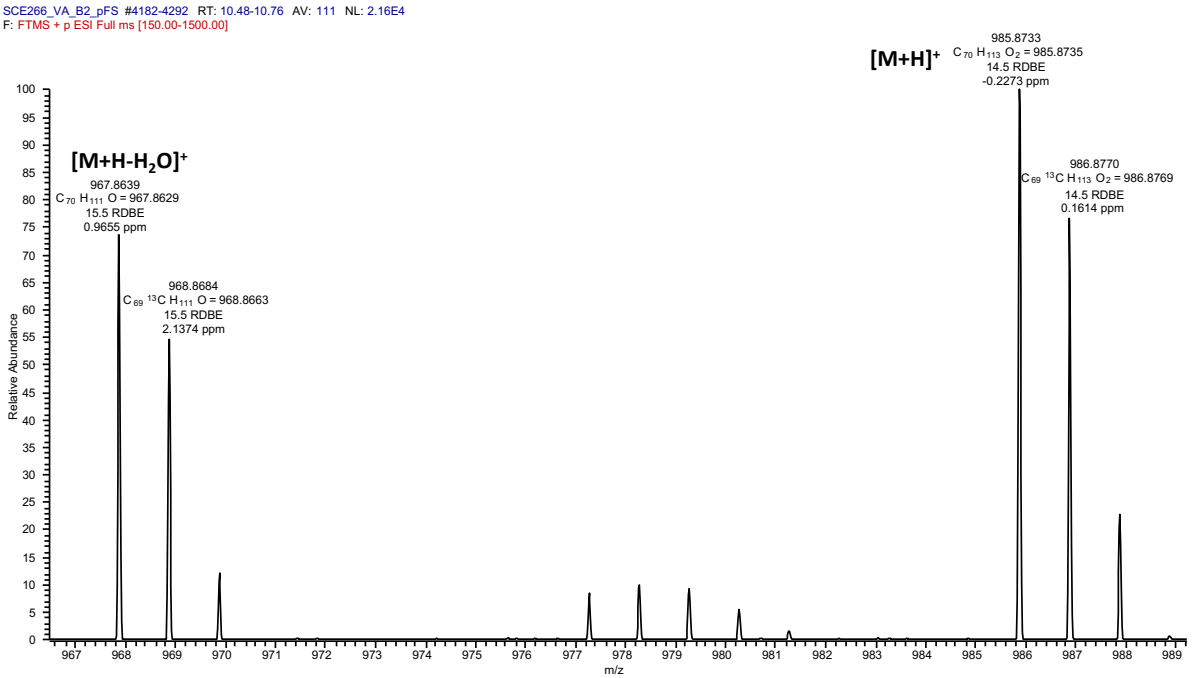

Figure S47. (+)-ESI-HRMS spectrum of the degradation fragments with elemental composition of $C_{70}H_{112}O_2$ obtained from C1.

Table S5. Degradation fragments produced by enzymatic cleavage by Lcp_{K30} according to ESI-TOF MS

m/z [M+Na+CH_3OH]$^+$ (calculated)	N 1 (measured) [*m/z*]	N 2 (measured) [*m/z*]	N 3 (measured) [*m/z*]	A 1 (measured) [*m/z*]	C 1 (measured) [*m/z*]	C 2 (measured) [*m/z*]	C 3 (measured) [*m/z*]
427.32	427.32	427.31	427.31	427.32	427.32	427.31	427.32
495.38	495.40	495.37	495.37	495.40	495.40	495.38	495.38
563.44	563.47	563.44	562.42	563.46	563.46	563.44	563.44
631.50	631.53	631.51	631.50	631.52	631.52	631.51	631.50
699.57	699.62	699.57	699.55	699.57	699.58	699.57	699.56
767.63	767.65	767.63	767.61	767.65	767.65	767.62	767.62
835.69	835.72	835.69	835.68	835.72	835.71	835.69	835.68
903.76	903.78	903.75	903.74	903.78	903.78	903.75	903.75
971.82	971.85	971.82	971.80	971.84	971.84	971.82	971.81

m/z [M+Na+CH_3OH]$^+$	Sample	
427	N 1	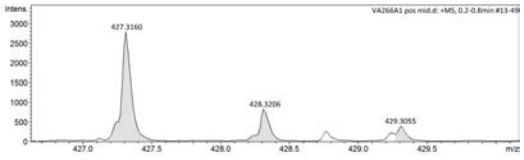
	N 2	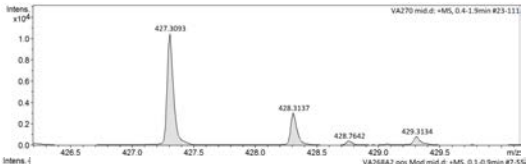
	N 3	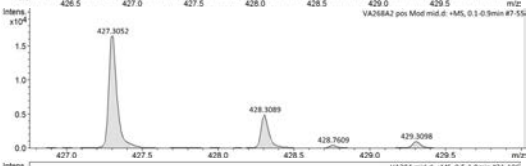
	A 1	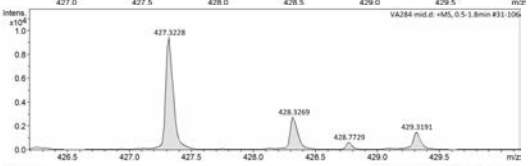
	C 1	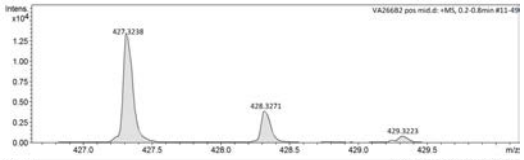
	C 2	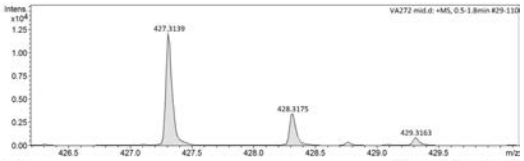
	C 3	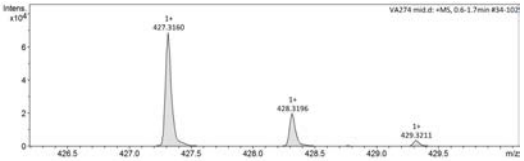
	Simulated pattern	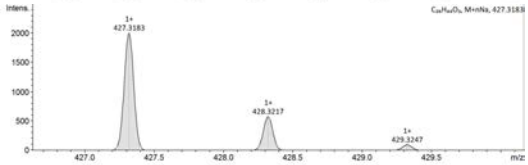

m/z $[M+Na+CH_3OH]^+$	Sample	
495	N 1	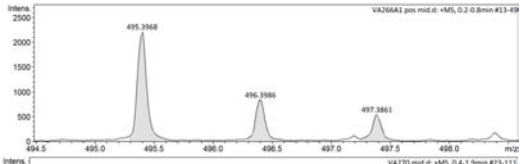
	N 2	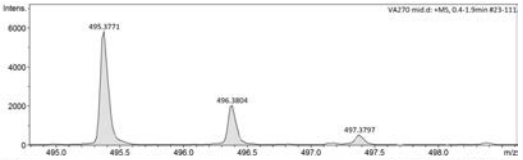
	N 3	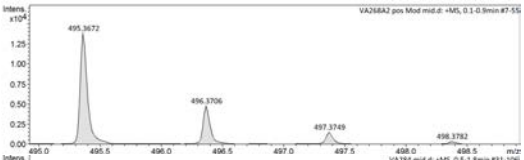
	A 1	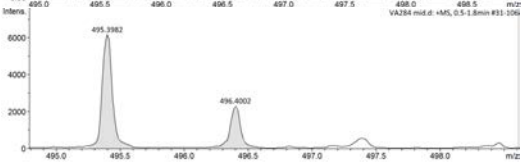
	C 1	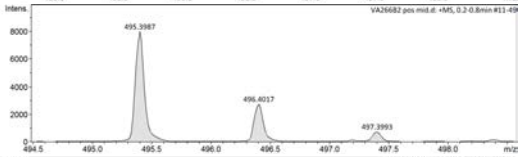
	C 2	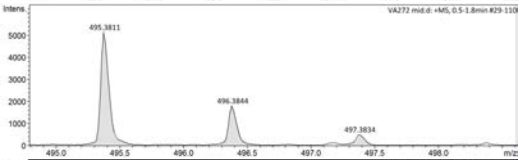
	C 3	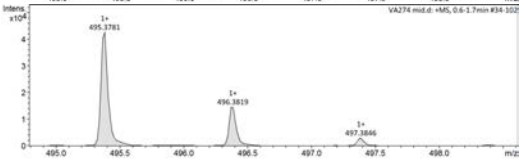
	Simulated pattern	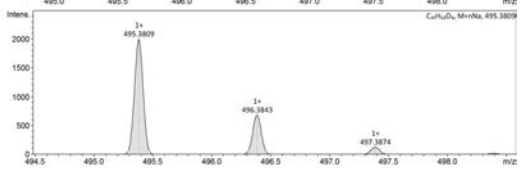

m/z $[M+Na+CH_3OH]^+$	Sample	
563	N 1	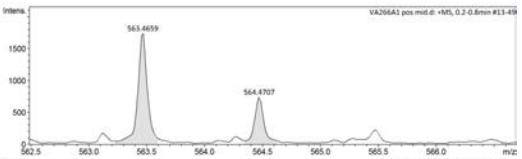
	N 2	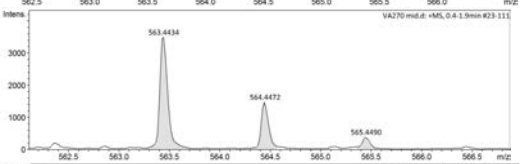
	N 3	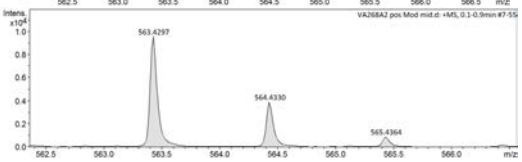

A 1

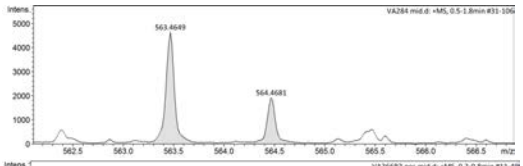

C 1

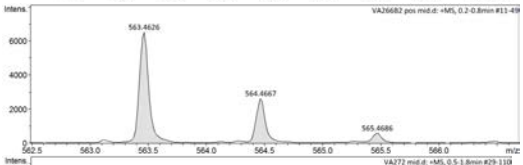

C 2

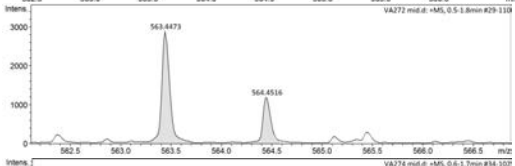

C 3

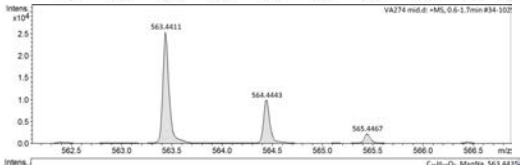

Simulated pattern

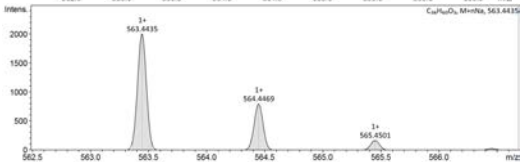

m/z $[M+Na+CH_3OH]^+$	Sample
631	N 1

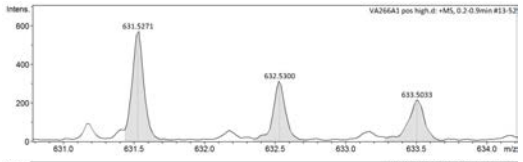

N 2

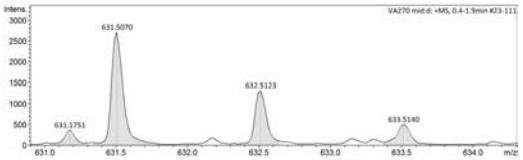

N 3

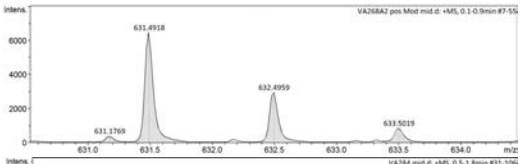

A 1

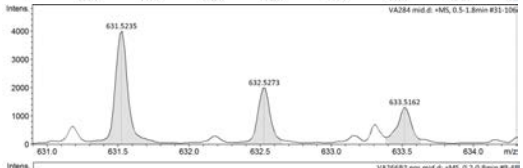

C 1

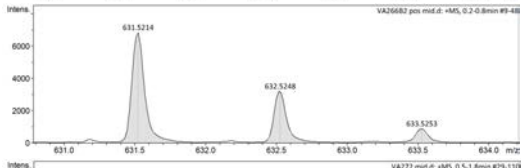

C 2

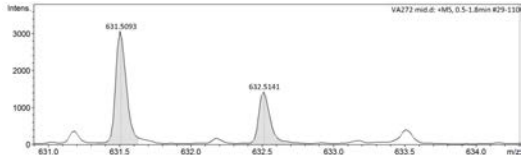

C 3

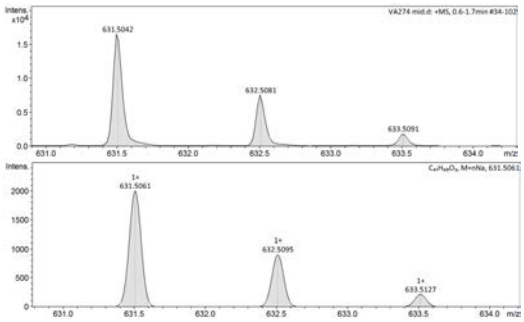

Simulated pattern

m/z $[M+Na+CH_3OH]^+$	Sample
699	N 1

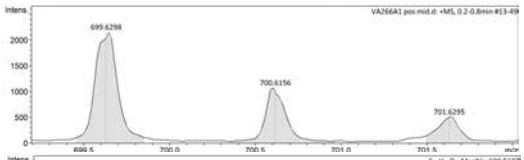

N 2

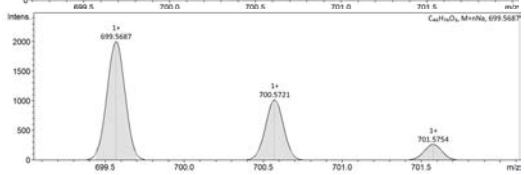

N 3

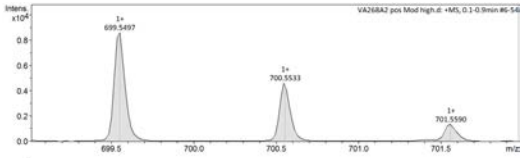

A 1

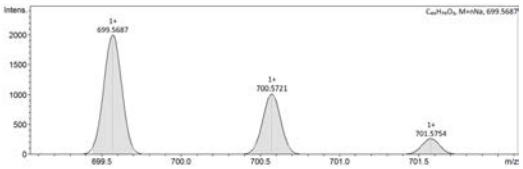

C1

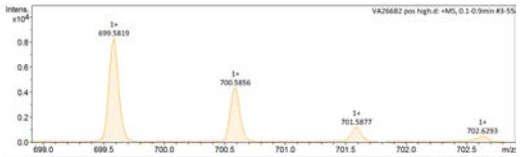

C 2

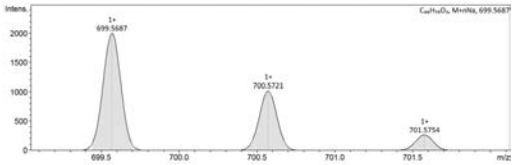

C 3

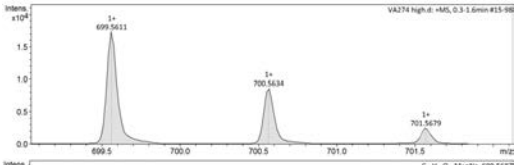

Simulated pattern

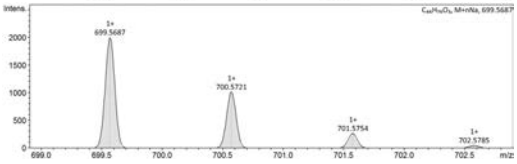

m/z $[M+Na+CH_3OH]^+$	Sample	
767	N 1	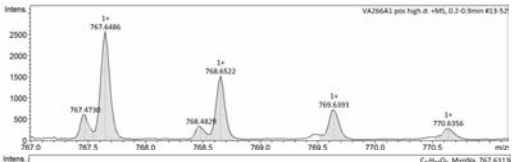
	N 2	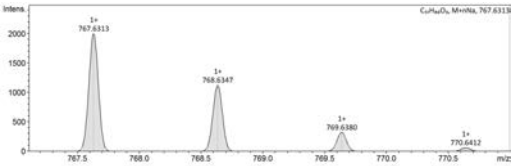
	N 3	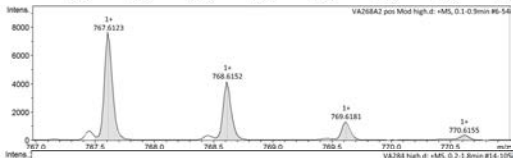
	A 1	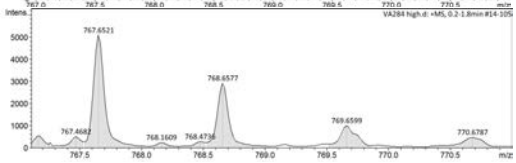
	C 1	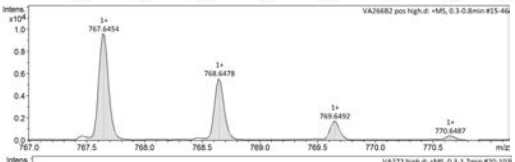
	C 2	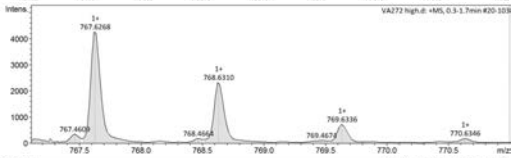
	C 3	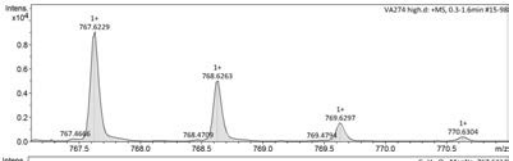
	Simulated pattern	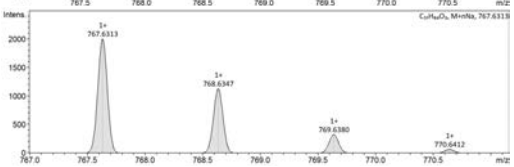

m/z $[M+Na+CH_3OH]^+$	Sample	
835	N 1	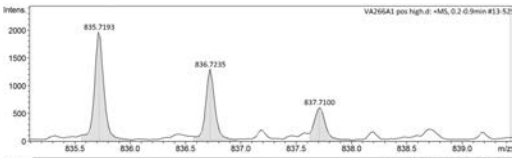
	N 2	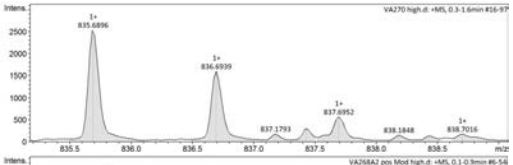
	N 3	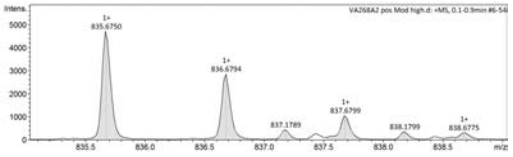

A 1

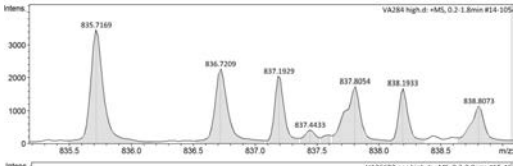

C 1

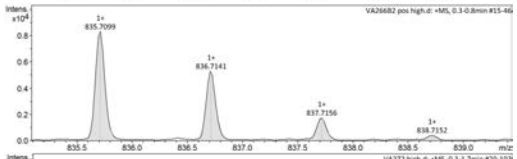

C 2

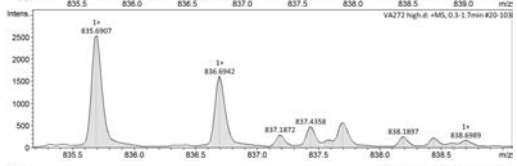

C 3

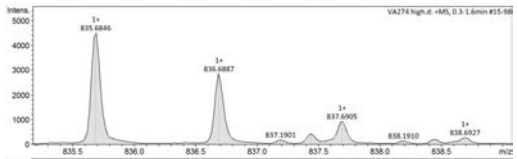

Simulated pattern

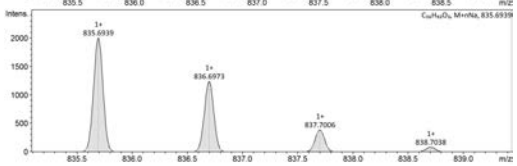

m/z $[M+Na+CH_3OH]^+$	Sample
903	N 1

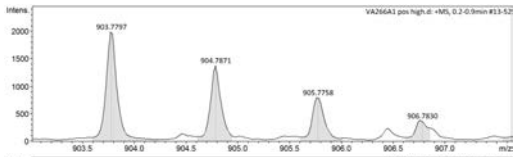

N 2

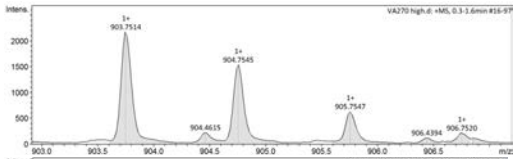

N 3

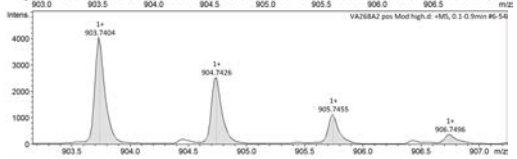

A 1

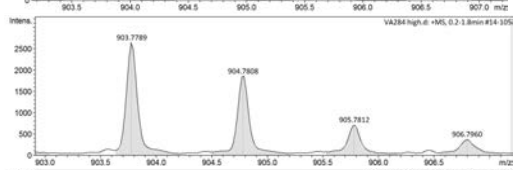

C 1

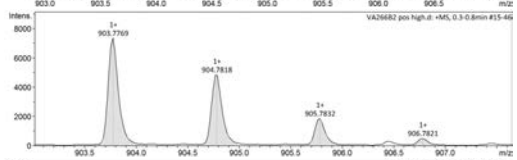

C 2

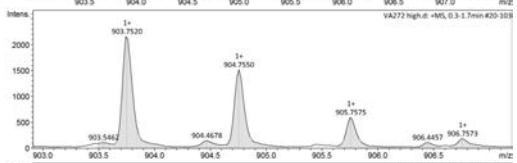

C 3

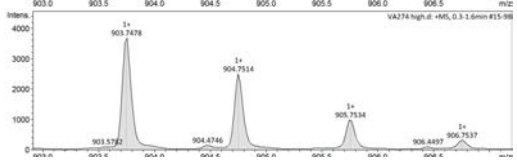

m/z [M+Na+CH_3OH]$^+$	Sample	
	Simulated pattern	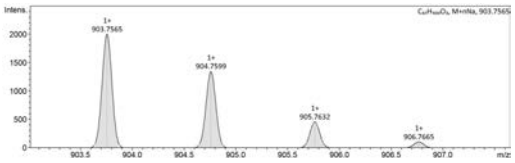
971	N 1	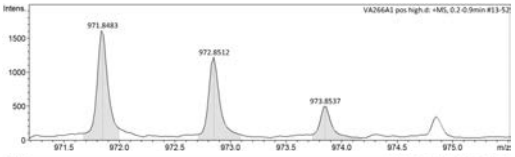
	N 2	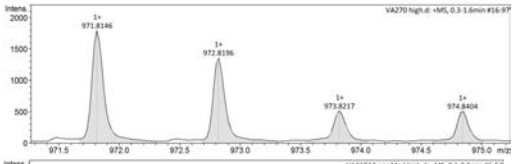
	N 3	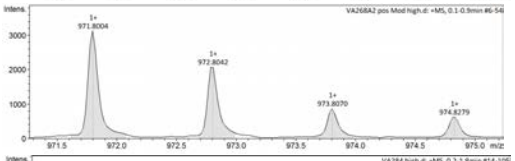
	A 1	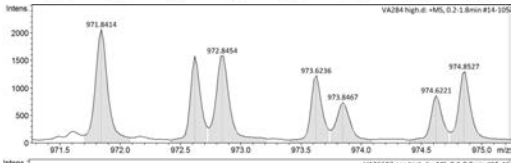
	C 1	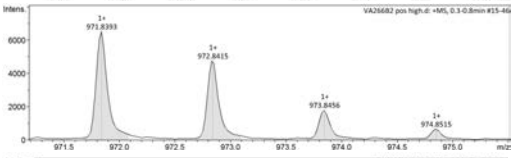
	C 2	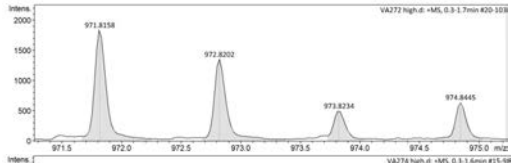
	C 3	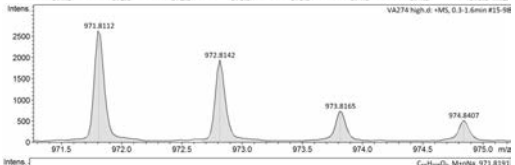
	Simulated pattern	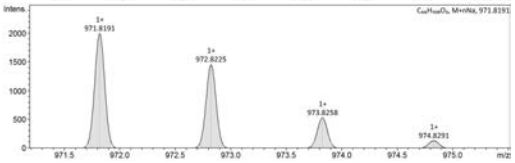

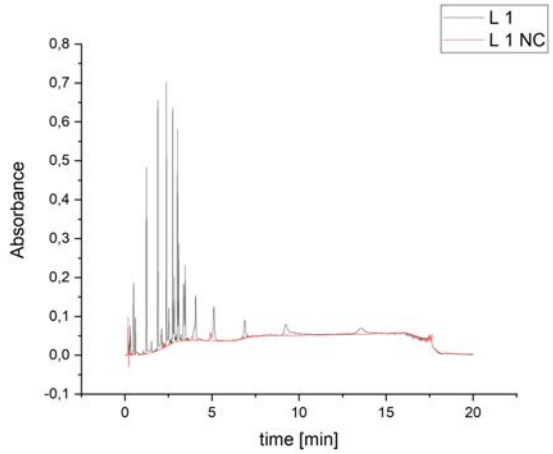

Figure S48. Separation of latex milk derived polyisoprene cleavage products (L 1; black) and negative control (L 1 NC; red) with UHPLC. UHPLC was conducted at conditions as seen above.

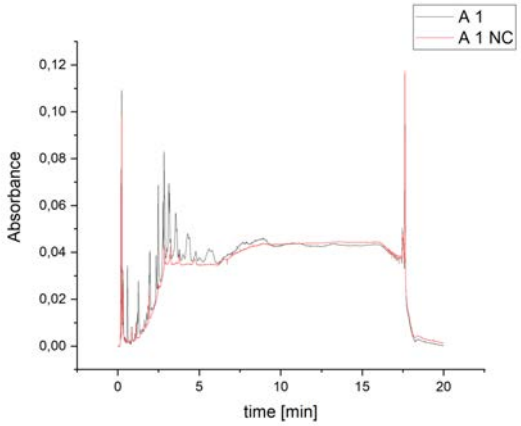

Figure S49. Separation of acoustically emulsified PI 3000 derived polyisoprene cleavage products (A 1; black) and negative control (A 1 NC; red) with UHPLC. UHPLC was conducted at conditions as seen above.

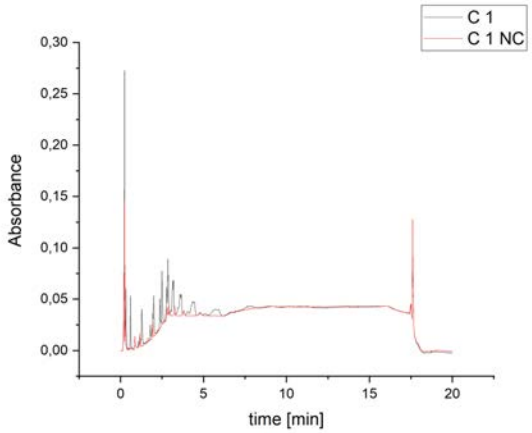

Figure S50. Separation of co-solvent stabilized PI 3000 derived polyisoprene cleavage products (C 1; black) and negative control (C 1 NC; red) with UHPLC. UHPLC was conducted at conditions as seen above.

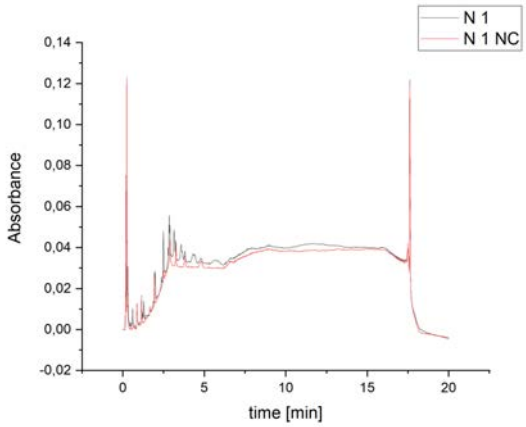

Figure S51. Separation of non-emulsified PI 3000 derived polyisoprene cleavage products (N 1; black) and negative control (N 1 NC; red) with UHPLC. UHPLC was conducted at conditions as seen above.

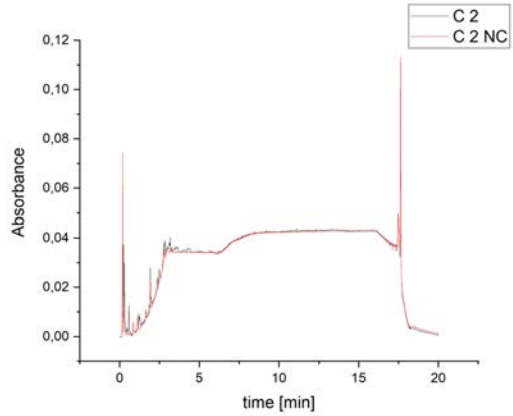

Figure S52. Separation of co-solvent stabilized PI 15 000 derived polyisoprene cleavage products (C 2; black) and negative control (C 2 NC; red) with UHPLC. UHPLC was conducted at conditions as seen above.

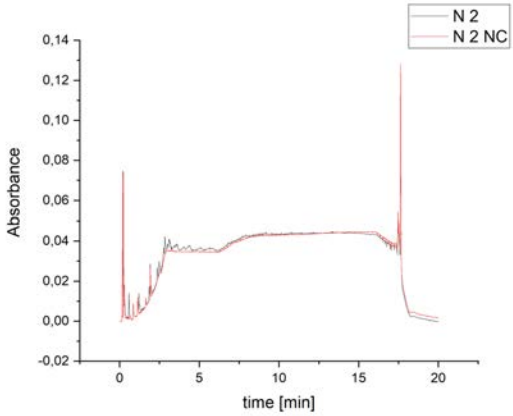

Figure S53. Separation of non-emulsified PI 15 000 derived polyisoprene cleavage products (N 2; black) and negative control (N 2 NC; red) with UHPLC. UHPLC was conducted at conditions as seen above.

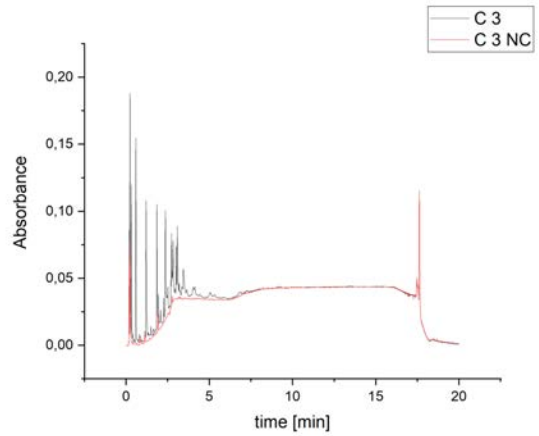

Figure S54. Separation of co-solvent stabilized PI *cis* 7000 derived polyisoprene cleavage products (C 3; black) and negative control (C 3 NC; red) with UHPLC. UHPLC was conducted at conditions as seen above.

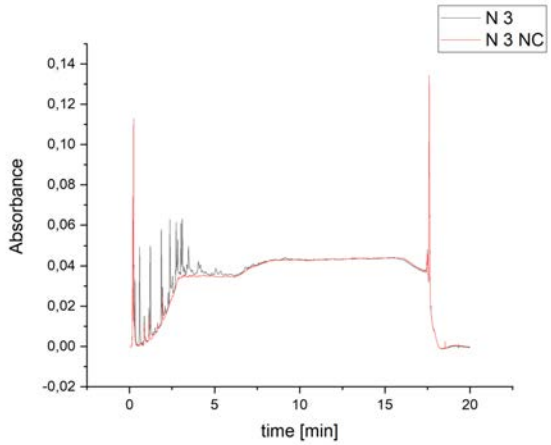

Figure S55. Separation of non-emulsified PI *cis* 7000 derived polyisoprene cleavage products (N 3; black) and negative control (N 3 NC; red) with UHPLC. UHPLC was conducted at conditions as seen above.

After liquid: liquid extraction the residue was extracted with *n*-hexane.
1.5 mL of *n*-hexane was added, sonicated for 10 minutes and stirred for 30 minutes. 1 mL of the *n*-hexane was extracted and used for analysis of the entire polymer backbone to investigate if the enzymatic degradation also led to a decrease of the overall number average molar mass of the residue polymer.

Table S6. GPC Triplicates.

Emulsification Strategy	Indicator	M_n (GPC)	M_w (GPC)	PDI
non emulsified:				
PI 3000	N 1	2300	3400	1.5
		2300	3400	1.5
		2200	3400	1.5
	N 1 NC	2200	3400	1.5
		2200	3400	1.5
		2200	3400	1.6
PI 15000	N 2	2700	13500	4.4
		3200	13800	4.1
		3300	14200	4.5
	N 2 NC	3100	14200	4.5
		3200	14200	4.4
		3300	14400	4.4
PI cis 7000	N 3	3800	36400	9.7
		3500	36000	10.2
		3600	37800	10.4
	N 3 NC	2900	36100	12.5
		3400	36700	10.9
		3600	39100	10.8
A:				
PI 3000	A 1	2000	3300	1.6
		1700	3000	1.8
		2000	3300	1.6
	A 1 NC	900	2300	2.4
		1900	3400	1.8
		1200	2700	2.2
PI 15 000	A 2*	700	1500	2.1
		600	1300	2.1
		600	1100	1.9
	A 2 NC*	600	1100	1.7
		1100	8500	7.6
		600	1400	2.2
C:				
PI 3000	C 1	900	2600	2.8
		1000	2700	2.7
		900	2600	2.9
	C 1 NC	1500	3200	2.0

		1100	3000	2.5
		1200	3000	2.4
PI 15000	C 2	4200	14100	3.4
		4300	14600	3.4
		3800	13900	3.6
	C 2 NC	4000	14900	4.0
		4600	15300	3.8
		3300	15800	3.4
PI cis 7000	C 3	3300	38100	11.6
		3600	39000	9.4
		3100	34000	11.2
	C 3 NC	3500	36500	10.4
		3400	36500	10.6
		3200	39100	12.1

*= acoustical emulsification of the entire PI 15 000 not successful.

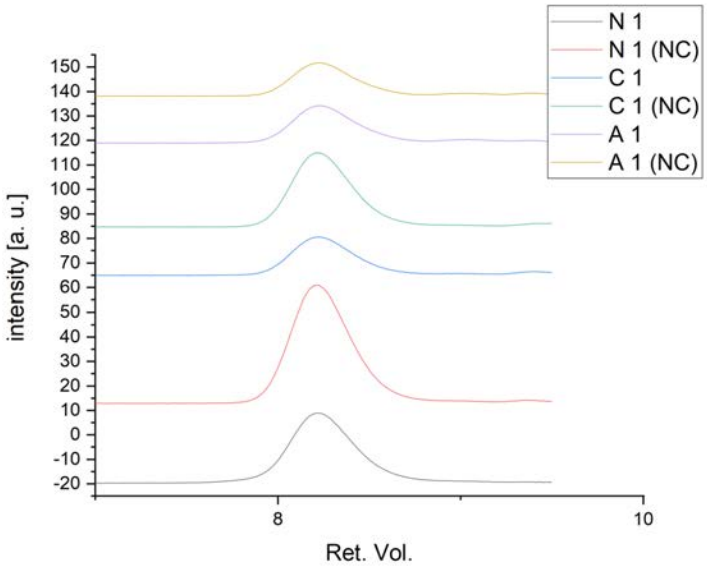

Figure S56. Stacked GPC traces of enzymatically degraded PI 3000 with corresponding negative controls without enzyme. (N 1=black, N 1 (NC)=red, C 1= blue, C 1 (NC)= green, A 1=purple and A 1 (NC) light brown)

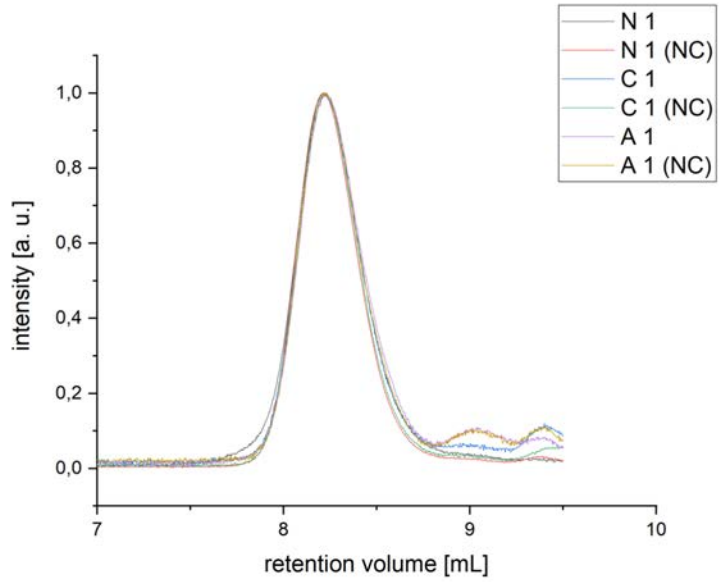

Figure S57. Stacked normalized GPC traces of traces of enzymatically degraded PI 3000 with corresponding negative controls without enzyme. (N 1=black, N 1 (NC)=red, C 1= blue, C 1 (NC)= green, A 1=purple and A 1 (NC) light brown)

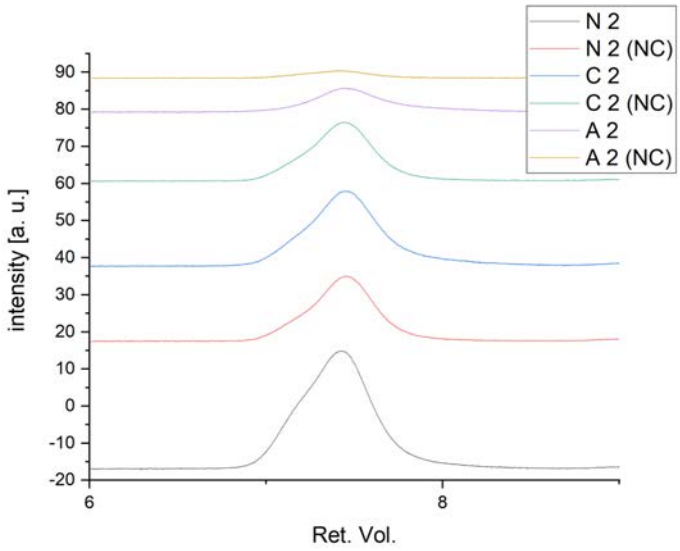

Figure S58. Stacked GPC traces of enzymatically degraded PI 15000 with corresponding negative controls without enzyme. (N 1=black, N 1 (NC)=red, C 1= blue, C 1 (NC)= green, A 1=purple and A 1 (NC) light brown)

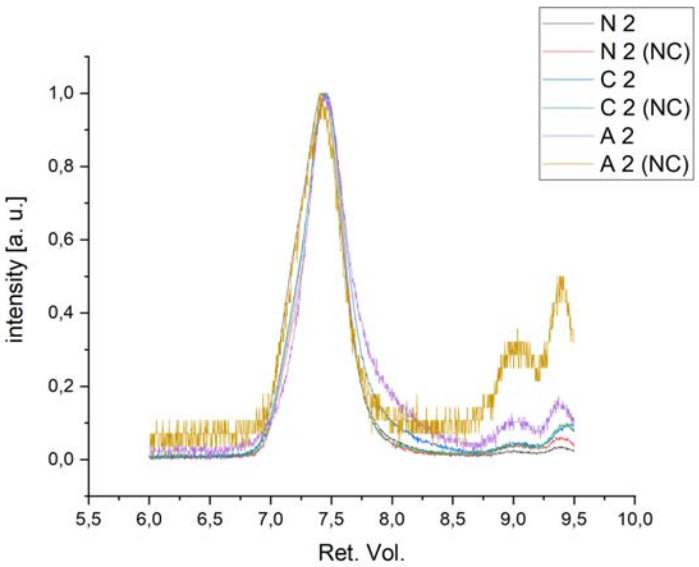

Figure S59. Stacked normalized GPC traces of enzymatically degraded PI 15000 with corresponding negative controls.of PI 15000 without enzyme. (N 1=black, N 1 (NC)=red, C 1= blue, C 1 (NC)= green, A 1=purple and A 1 (NC) light brown)

6. References

1. P. Pullmann, C. Ulpinnis, S. Marillonnet, R. Gruetzner, S. Neumannand M. J. Weissenborn, *Sci. Rep.* 2019, **9**, 10932.
2. S. Cabantous and G. S. Waldo, *Nat. Methods* 2006, **3**, 845-854.
3. L. Ilcu, W. Rother, J. Birke, A. Brausemann, O. Einsle and D. Jendrossek, *Sci. Rep.* 2017,**7**, 6179.
4. D. Jendrossek and J. Birke*, Appl. Microbiol. Biotechnol.*, 2019, **103**, 125-142.
5. W. Rother, J. Birke, S. Grond, J. M. Beltran and D. Jendrossek, *Microb. Biotechnol.*, 2017, **10**, 1426-1433.
6. R. Andler, A.Steinbüchel, *J. Biotechnol.*, 2017, **241**, 184-192.
7. S. Hiessl, D. Böse, S. Oetermann, J. Eggers, J. Pietruszka, A. Steinbüchel*, Appl. Environ. Microbiol.* 2014, **80**, 5231-5240.
8. F. Sadaka, I. Campistron, A. Laguerre, J.-F.Pilard, *Polym. Degrad. Stab.* 2012, **97**, 816-828.